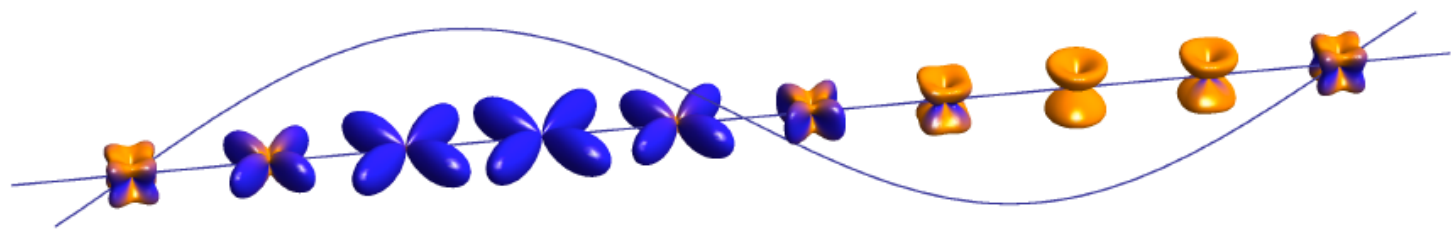
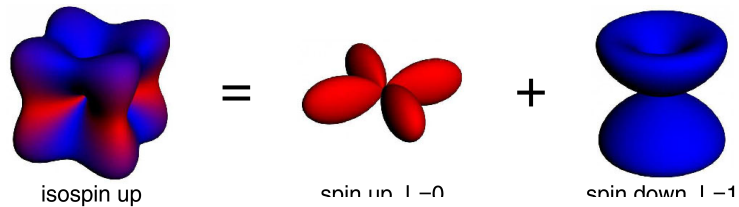


Resonant X-ray Scattering: Application to Iridates

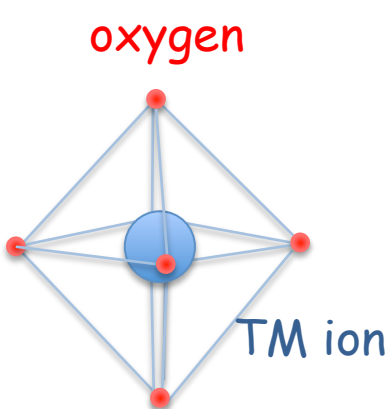
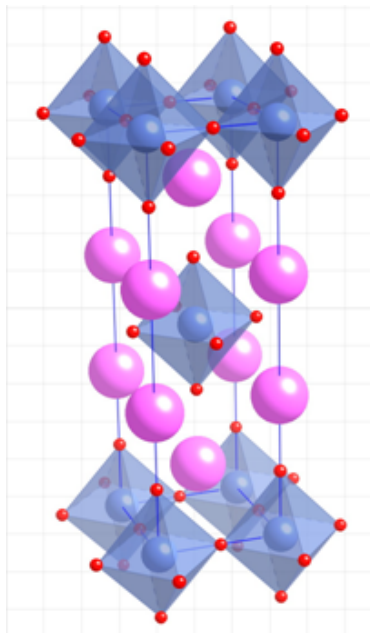


B. J. Kim

Max Planck Institute for Solid State Research

Transition metal oxides: Diverse Properties

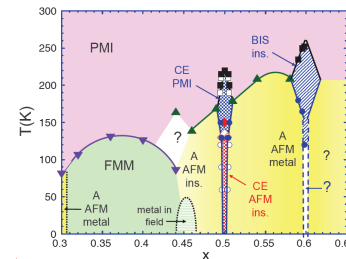
(Layered) Perovskite structure



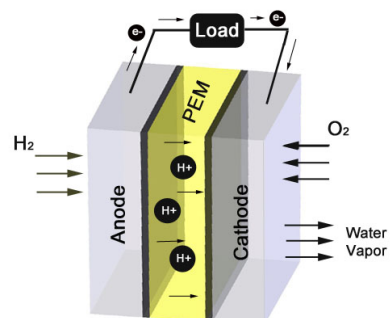
Cu: high-T_c superconductivity



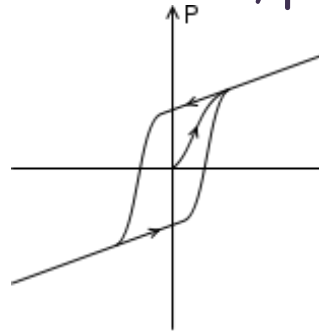
Mn: Colossal magnetoresistance



Ni: Fuel cell cathodes

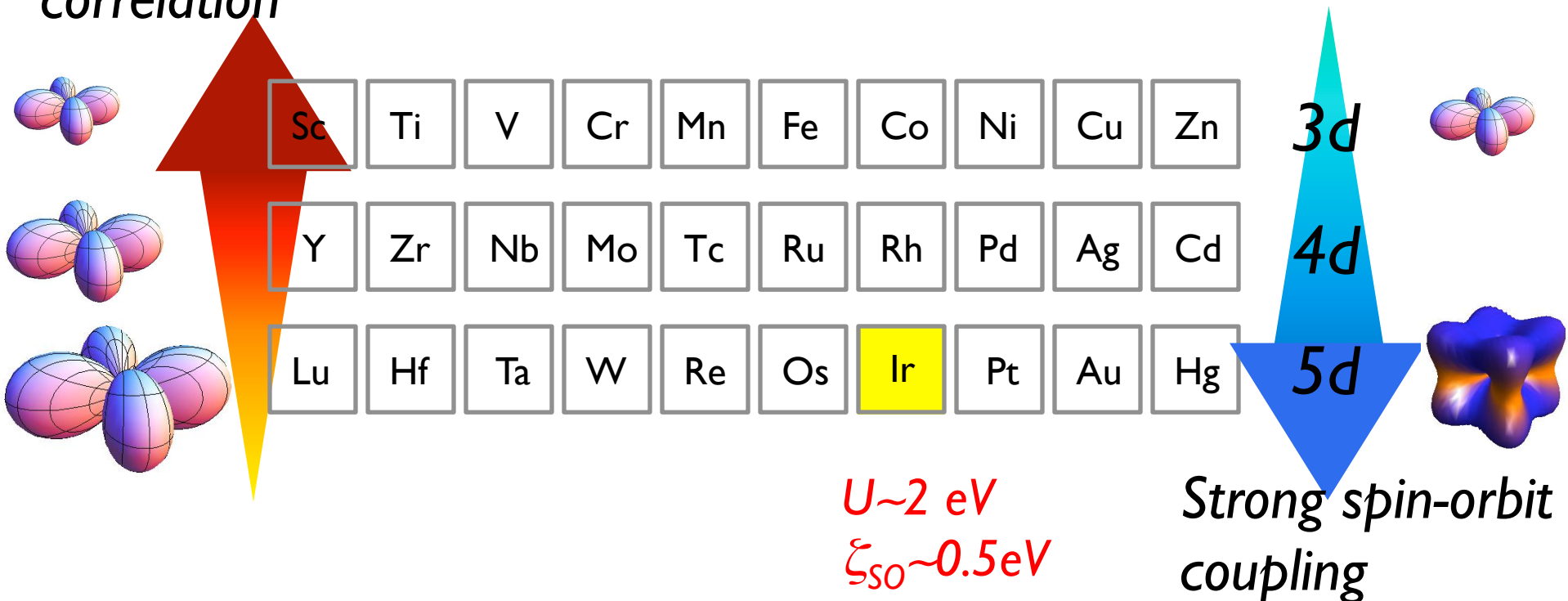


Ti: ferroelectric, piezoelectric

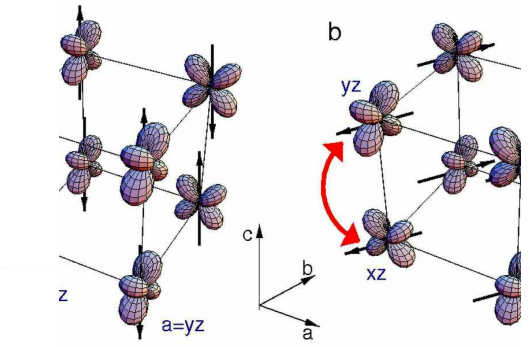


Transition metal oxides

Strong electron correlation

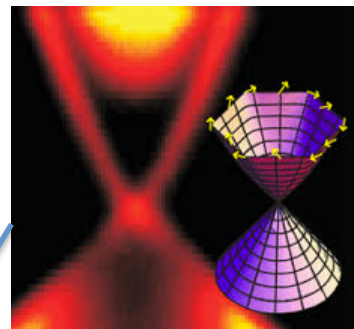


Correlation + Spin-Orbit Coupling



- high T_c superconductivity
- colossal magnetoresistance

3	4	5	6	7	8	9	10	11	12
scandium 21	titanium 22	vandium 23	chromium 24	manganese 25	iron 26	cobalt 27	nickel 28	copper 29	zinc 30
44.966	47.967	50.942	51.996	54.938	55.845	58.933	58.693	63.546	65.39
yttrium 39	zirconium 40	niobium Nb	molybdenum Mo	technetium 43	ruthenium 44	rhenium [96]	rhodium 45	palladium 46	silver 47
88.906	91.224	92.906	95.94	101.07	102.91	101.97	106.42	107.87	112.41
lutetium 71	hafnium 72	tantalum 73	tungsten 74	rhenium 75	osmium 76	iridium 77	platinum 78	gold 79	mercury 80
174.97	178.49	180.95	183.84	186.21	190.23	192.22	195.08	196.97	200.59
lawrencium 103	rutherfordium 104	dubnium 105	seaborgium 106	bohrium 107	hassium 108	meitnerium 109	darmstadium 110	roentgenium 111	ununbium 112
[262]	[261]	[262]	[263]	[269]	[269]	[269]	[271]	[272]	[277]
lanthanum 57	cerium 58	praseodymium 59	neodymium 60	promethium 61	samarium 62	europlum 63	gadolinium 64	terbium 65	dysprosium 66
La 138.91	Ce 140.12	Pr 140.91	Nd 144.24	Pm [145]	Sm 150.36	Eu 151.96	Gd 157.25	Tb 158.93	Dy 162.50
actinium 89	thorium 90	protactinium 92	uranium U	neptunium 93	plutonium 94	americium 95	curium 96	berkelium 97	californium 98
Ac [227]	Th 232.04	Pa 231.04	[238.03]	[237]	[244]	[243]	[247]	[247]	[251]

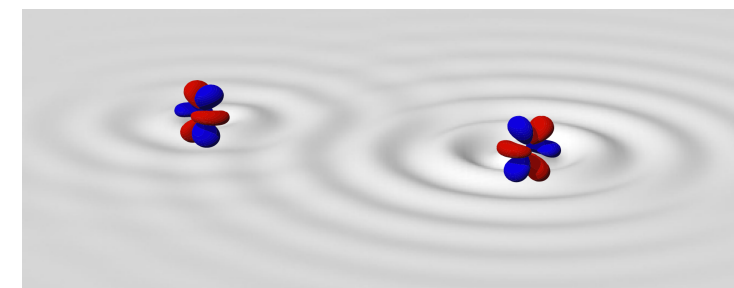


- topological insulator

- novel topological phases
- Kitaev quantum spin liquid
- unconventional superconductivity

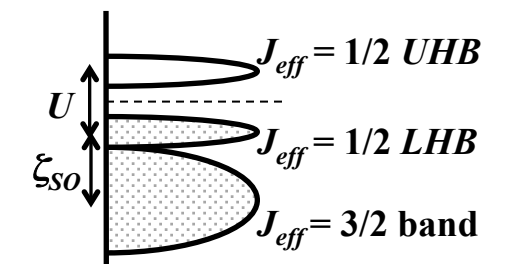
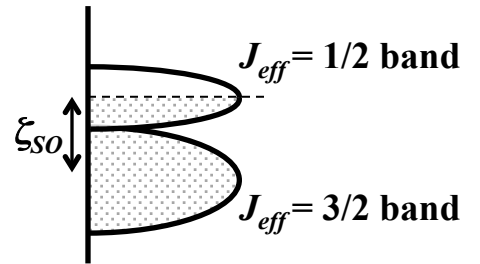
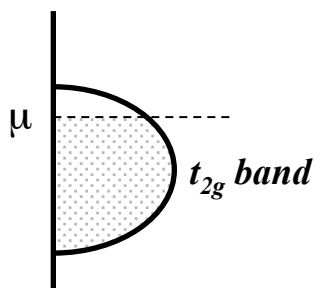
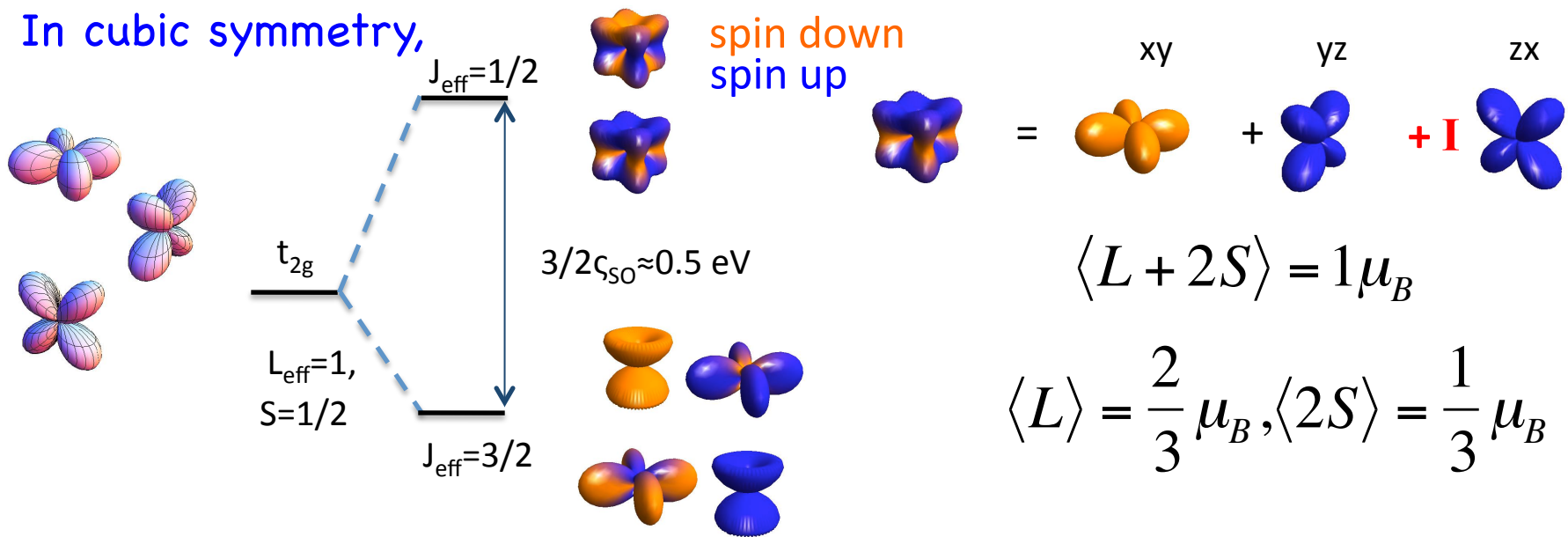
lanthanum 57	cerium 58	praseodymium 59	neodymium 60	promethium 61	samarium 62	europlum 63	gadolinium 64	terbium 65	dysprosium 66	holmium 67	erbium 68	thulium 69	yterbium 70	ytterbium Yb
La 138.91	Ce 140.12	Pr 140.91	Nd 144.24	Pm [145]	Sm 150.36	Eu 151.96	Gd 157.25	Tb 158.93	Dy 162.50	Ho 164.93	Er 167.26	Tm 168.93	[173.04]	
actinium 89	thorium 90	protactinium 92	uranium U	neptunium 93	plutonium 94	americium 95	curium 96	berkelium 97	californium 98	einsteinium 99	fermium 100	mendelevium 101	nobelium 102	No
Ac [227]	Th 232.04	Pa 231.04	[238.03]	[237]	[244]	[243]	[247]	[247]	[251]	[252]	[257]	[258]	[259]	

- Kondo physics
- heavy fermion



SOC Induced Mott Transition

In cubic symmetry,



$J_{eff}=1/2$ states

t_{2g} maps onto $p(l=1, s=1/2)$ manifold (TP equivalence)

Taking only the t_{2g} subspace, angular momentum operator \mathbf{L} is given by

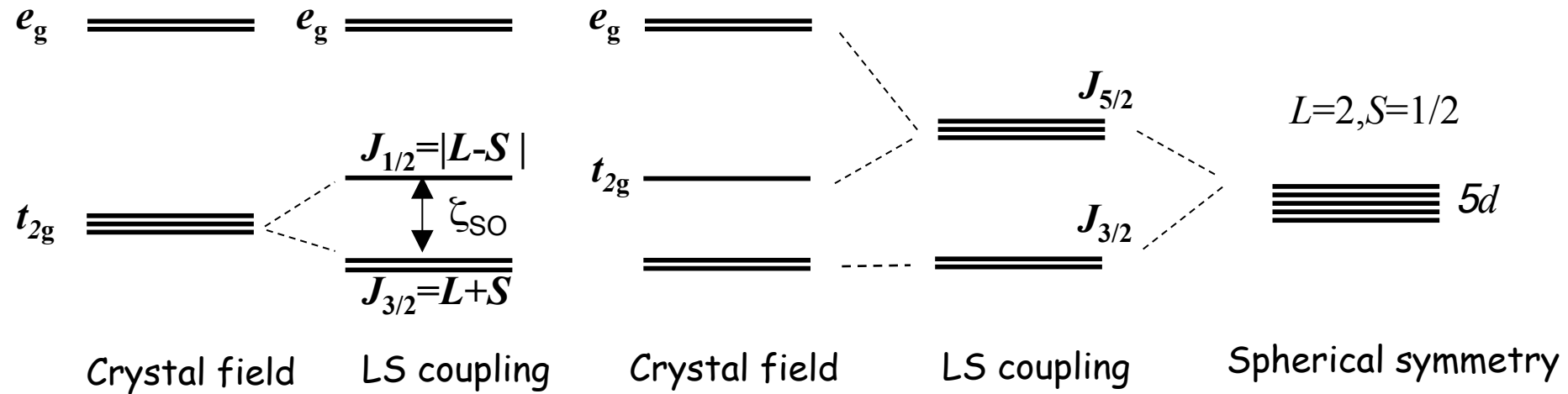
$$xy \quad yz \quad zx$$

$$L_x = \begin{pmatrix} 0 & 0 & -i \\ 0 & 0 & 0 \\ i & 0 & 0 \end{pmatrix} \quad L_y = \begin{pmatrix} 0 & i & 0 \\ -i & 0 & 0 \\ 0 & 0 & 0 \end{pmatrix} \quad L_z = \begin{pmatrix} 0 & 0 & 0 \\ 0 & 0 & i \\ 0 & -i & 0 \end{pmatrix}$$

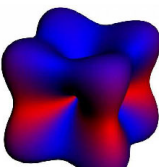
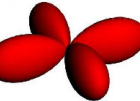
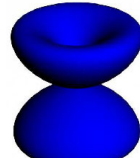
which can be mapped onto $L=1$ manifold with

$$p_z \rightarrow xy, p_x \rightarrow yz, p_y \rightarrow zx$$

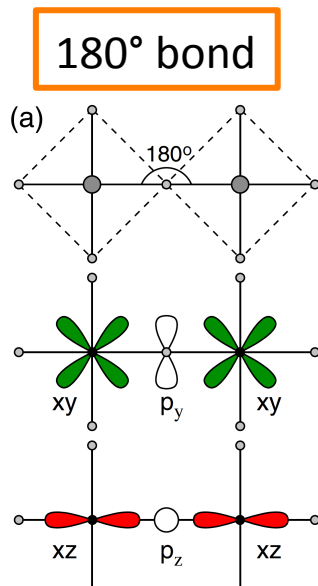
$$\mathbf{L}_{t_{2g}} \rightarrow -\mathbf{L}_p$$



Goodenough-Kanamori theory on $J_{\text{eff}}=1/2$ states

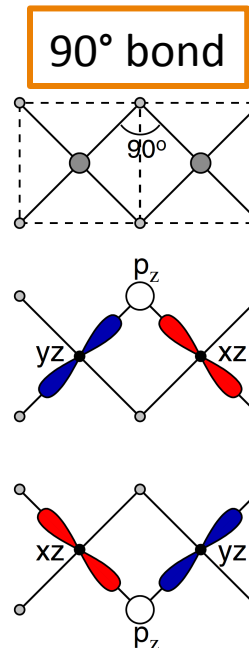
$J_{\text{eff}}=1/2$ states =  +  + 

$$|xy \uparrow\rangle + |yz \downarrow\rangle + i|zx \downarrow\rangle$$



Heisenberg

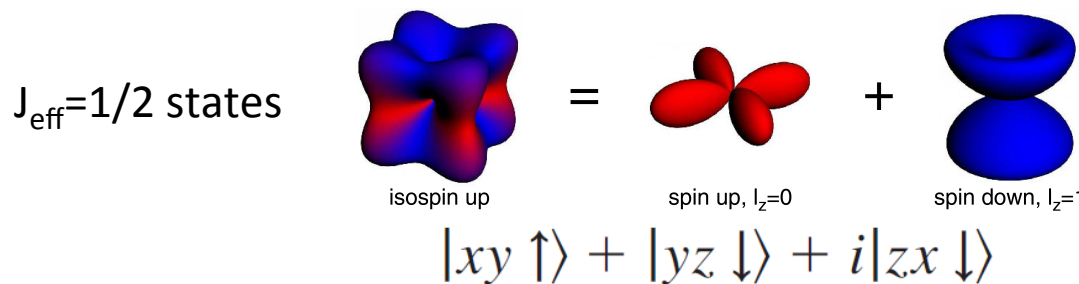
High-Tc superconductivity?



complete suppression of Heisenberg

Kitaev spin liquid?

Goodenough-Kanamori theory on $J_{\text{eff}}=1/2$ states



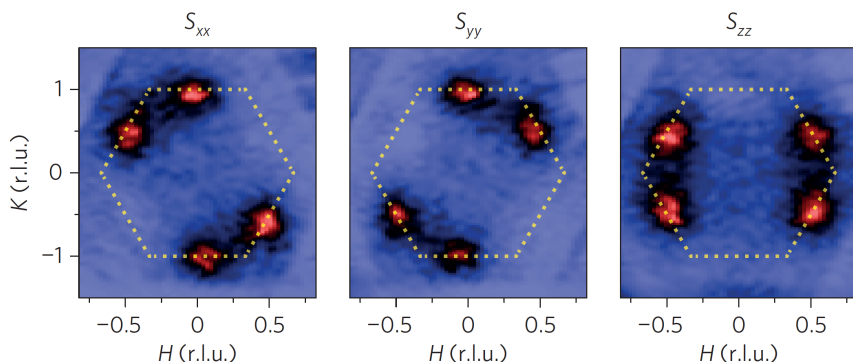
nature
physics

LETTERS

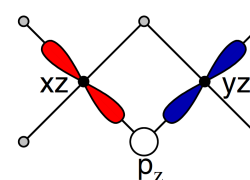
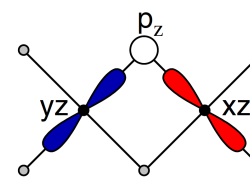
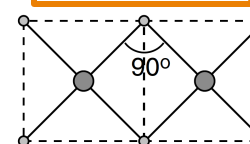
PUBLISHED ONLINE: 11 MAY 2015 | DOI: 10.1038/NPHYS3322

Direct evidence for dominant bond-directional interactions in a honeycomb lattice iridate Na_2IrO_3

Sae Hwan Chun¹, Jong-Woo Kim², Jungho Kim², H. Zheng¹, Constantinos C. Stoumpos¹, C. D. Malliakas¹, J. F. Mitchell¹, Kavita Mehlawat³, Yogesh Singh³, Y. Choi², T. Gog², A. Al-Zein⁴, M. Moretti Sala⁴, M. Krisch⁴, J. Chaloupka⁵, G. Jackeli^{6,7}, G. Khaliullin⁶ and B. J. Kim^{6*}

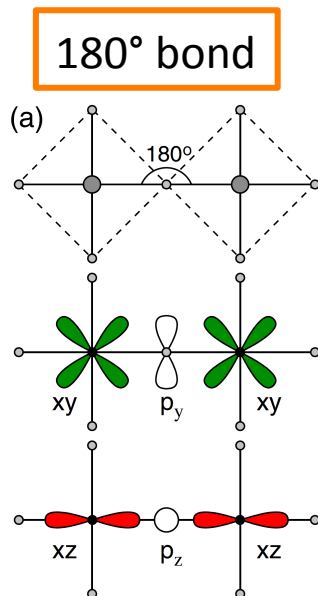
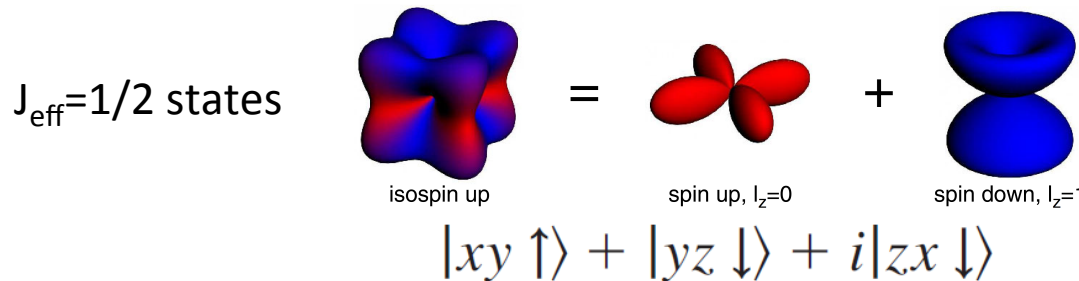


90° bond



complete suppression of Heisenberg
Kitaev spin liquid?

Goodenough-Kanamori theory on $J_{\text{eff}}=1/2$ states



Heisenberg

High-Tc superconductivity?

SUPERCONDUCTIVITY

Fermi arcs in a doped pseudospin-1/2 Heisenberg antiferromagnet

Y. K. Kim,¹ O. Krupin,¹ J. D. Denlinger,¹ A. Bostwick,¹ E. Rotenberg,¹ Q. Zhao,² J. F. Mitchell,² J. W. Allen,³ B. J. Kim^{2,3,4*}

arXiv.org > cond-mat > arXiv:1506.06639

Condensed Matter > Strongly Correlated Electrons

Observation of a d -wave gap in electron-doped Sr_2IrO_4

Y. K. Kim, N. H. Sung, J. D. Denlinger, B. J. Kim

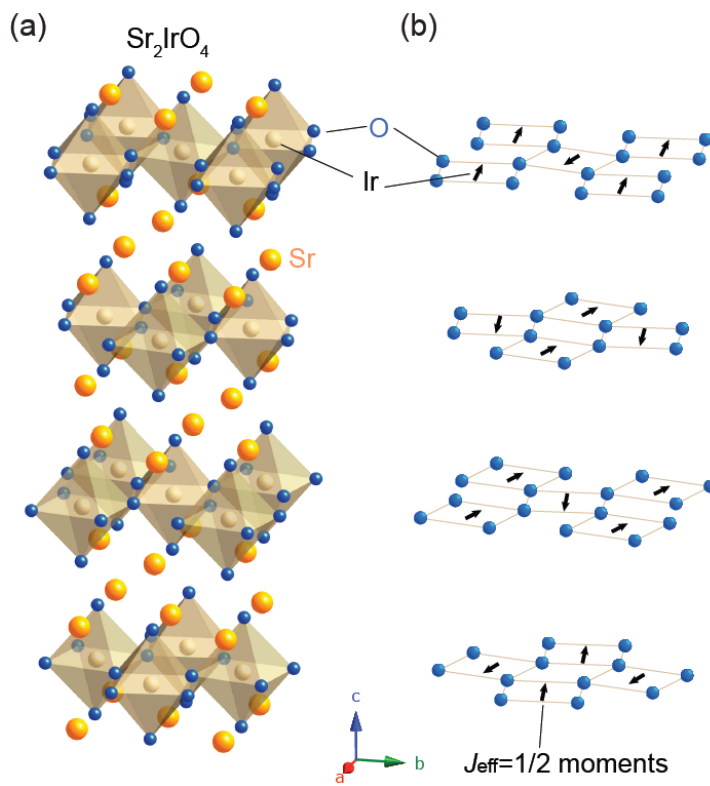
(Submitted on 22 Jun 2015 (v1), last revised 25 Jun 2015 (this version, v2))

High temperature superconductivity in cuprates emerges out of a highly enigmatic ‘pseudogap’ metal phase. The mechanism of high temperature superconductivity is likely encrypted in the elusive relationship between the two phases, which spectroscopically is manifested as Fermi arcs---disconnected segments of zero-energy states---collapsing into d -wave point nodes upon entering the superconducting phase. Here, we reproduce this distinct cuprate phenomenology in the 5d transition-metal oxide Sr_2IrO_4 . Using angle-resolved photoemission, we show that clean, low-temperature phase of 6–8% electron-doped Sr_2IrO_4 has gapless excitations only at four isolated points in the Brillouin zone with a predominant d -wave symmetry of the gap. Our work thus establishes a connection between the low-temperature d -wave instability and the previously reported high-temperature Fermi arcs in electron-doped Sr_2IrO_4 . Although the physical origin of the d -wave gap remains to be understood, Sr_2IrO_4 is a first non-cuprate material to spectroscopically reproduce the complete phenomenology of the cuprates, thus offering a new material platform to investigate the relationship between the pseudogap and the d -wave gap.

Ruddelsden-Popper Series Iridates



$T_N=240 \text{ K}$

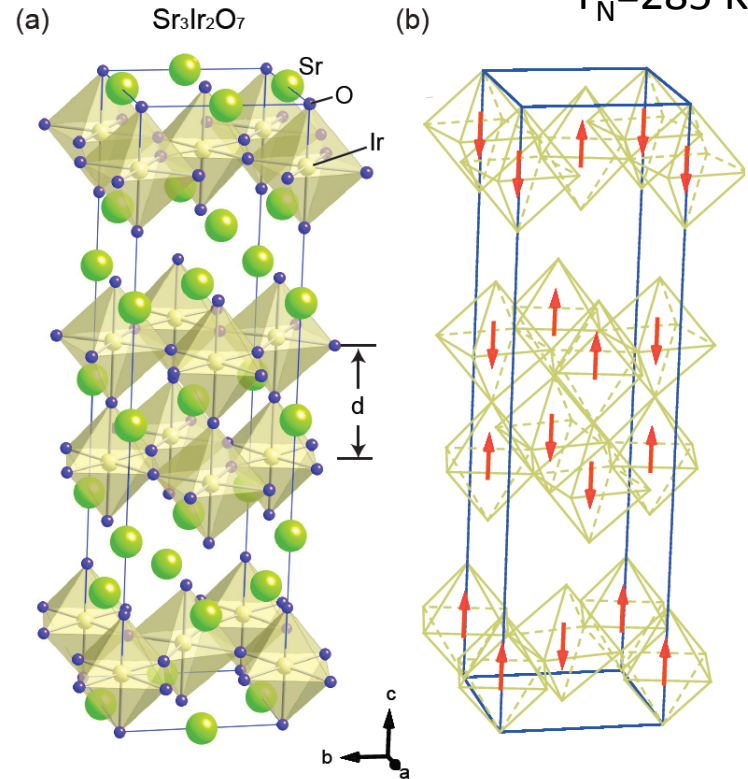


canted AF with
in-plane moments

B. J. Kim et al. Science (2009)



$T_N=285 \text{ K}$



G-type AF
c-axis collinear

J. -W. Kim, BJK et al. PRL (2012),
S. Boseggia et al, J. Phys. Condens. Matter (2015)
J. P. Clancy et al., arxiv (2012)
S. Fujiyama et al. PRB (2012)

Resonant x-ray scattering

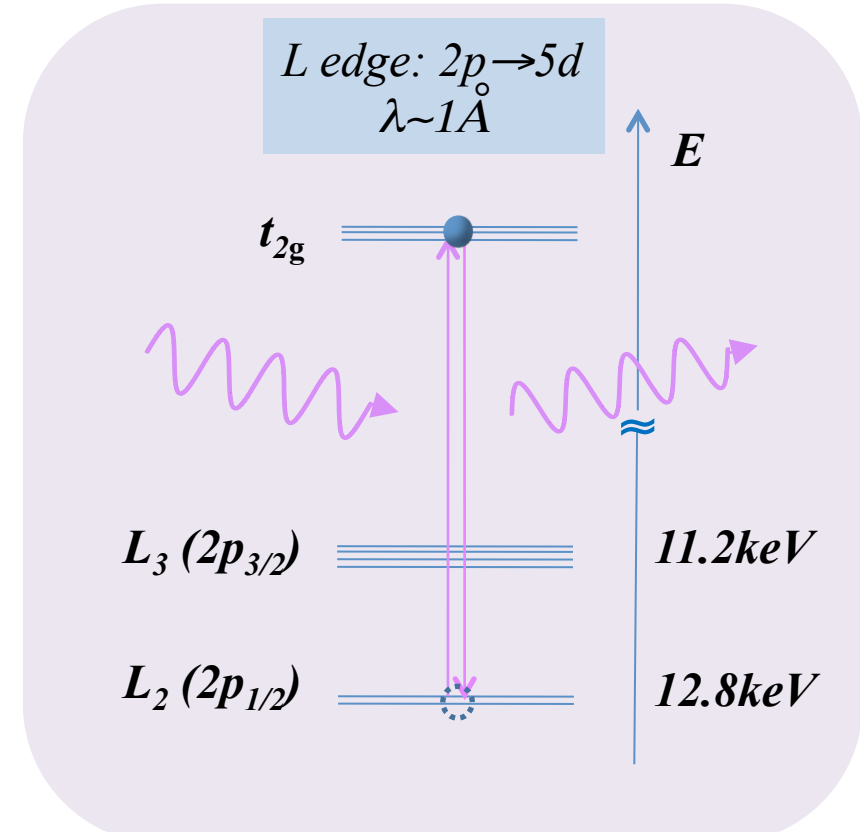
Direct probe for the 5d state responsible for magnetism

$$H' = \frac{e^2}{2m_e c^2} \sum_i A(\mathbf{r}_i)^2 - \frac{e^2 \hbar}{2m_e^2 c^4} \sum_i \mathbf{s}_i \cdot \left(\frac{\partial \mathbf{A}}{\partial t} \times \mathbf{A} \right) - \frac{e}{m_e c} \sum_i \mathbf{A}(\mathbf{r}_i) \cdot \mathbf{p} - \frac{e^2 \hbar}{2m_e^2 c^4} \sum_i \mathbf{s}_i \cdot (\nabla \times \mathbf{A}(\mathbf{r}_i))$$

$$F_{E1}^{(reso)} = \frac{e^2}{m_e c^2} \sum_{\mathbf{n}, \mathbf{m}} e^{i\mathbf{K} \cdot (\mathbf{n} + \mathbf{d}_m)} \sum_{\alpha\beta} \epsilon'_\alpha \epsilon_\beta f_m^{\alpha\beta}$$

$$f_m^{\alpha\beta} = \sum_c \frac{m_e \omega_{ca}^3}{\omega} \frac{\langle a | R_m^\alpha | c \rangle \langle c | R_m^\beta | a \rangle}{\hbar\omega - \hbar\omega_{ac} + i\Gamma/2}$$

Cartesian tensor of rank 2



Resonant x-ray scattering and x-ray absorption

-Related through the optical theorem

$$\begin{aligned} F_{\epsilon_{in}\epsilon_{out}} &= F^{(0)}(\epsilon_{in} \cdot \epsilon_{out}^*) && \text{charge} \\ &+ F^{(1)}(\epsilon_{in} \times \epsilon_{out}^* \cdot \hat{m}) && \text{magnetic dipole} \\ &+ F^{(2)}((\epsilon_{out}^* \cdot \hat{m})(\epsilon_{in} \cdot \hat{m}) - \frac{1}{3}(\epsilon_{in} \cdot \epsilon_{out}^*)) && \text{electric quadrupole} \end{aligned}$$

F^0 , describes the isotropic absorption

F^1 , describes the XMCD spectra

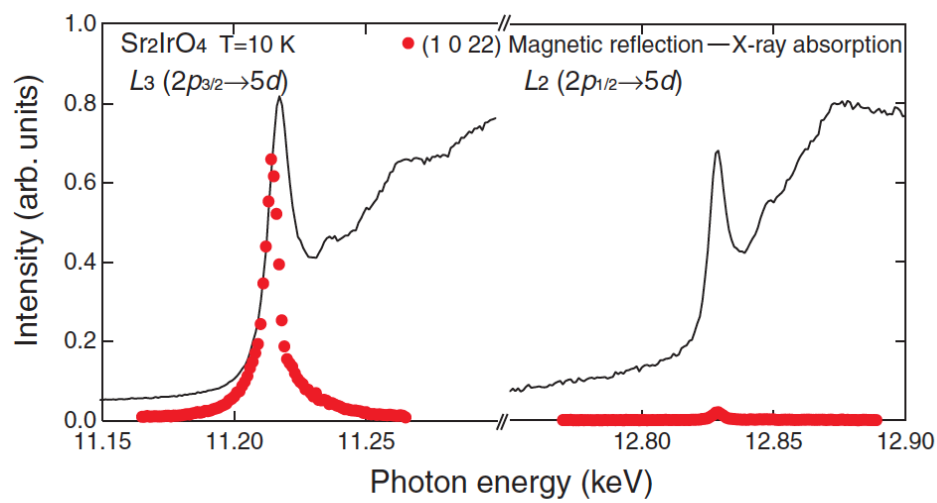
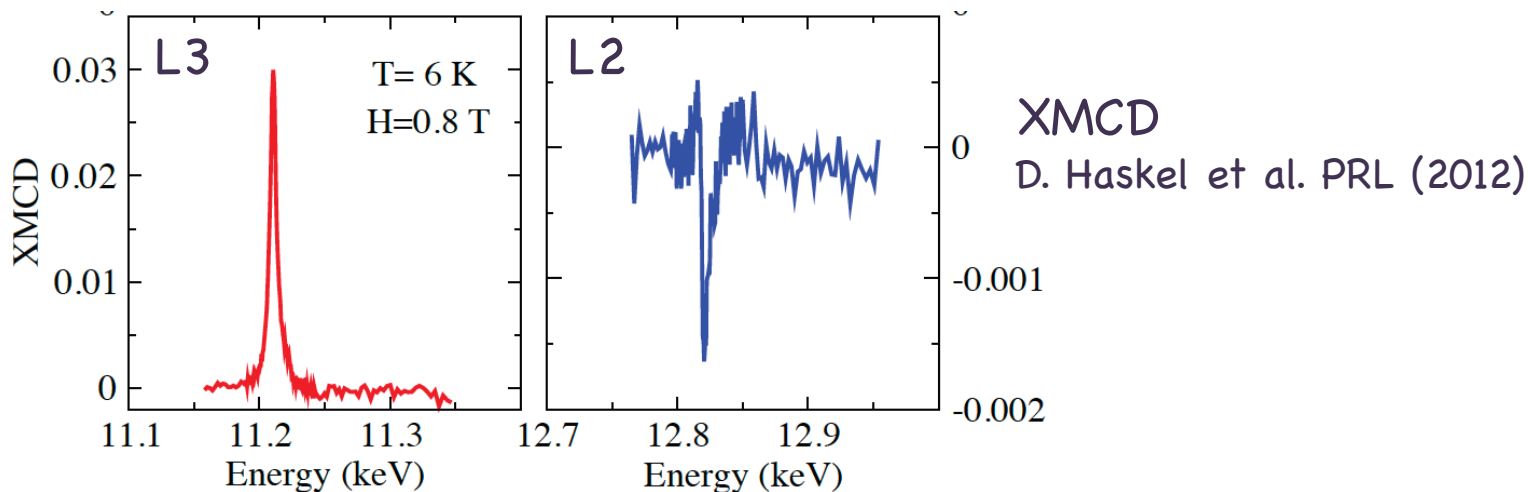
F^2 , describes the XMLD spectra

G. van der Laan, J. Phys. Soc. Jpn. 63, 2393 (1994)

M. Haverkort, PRL 105, 167404 (2010)

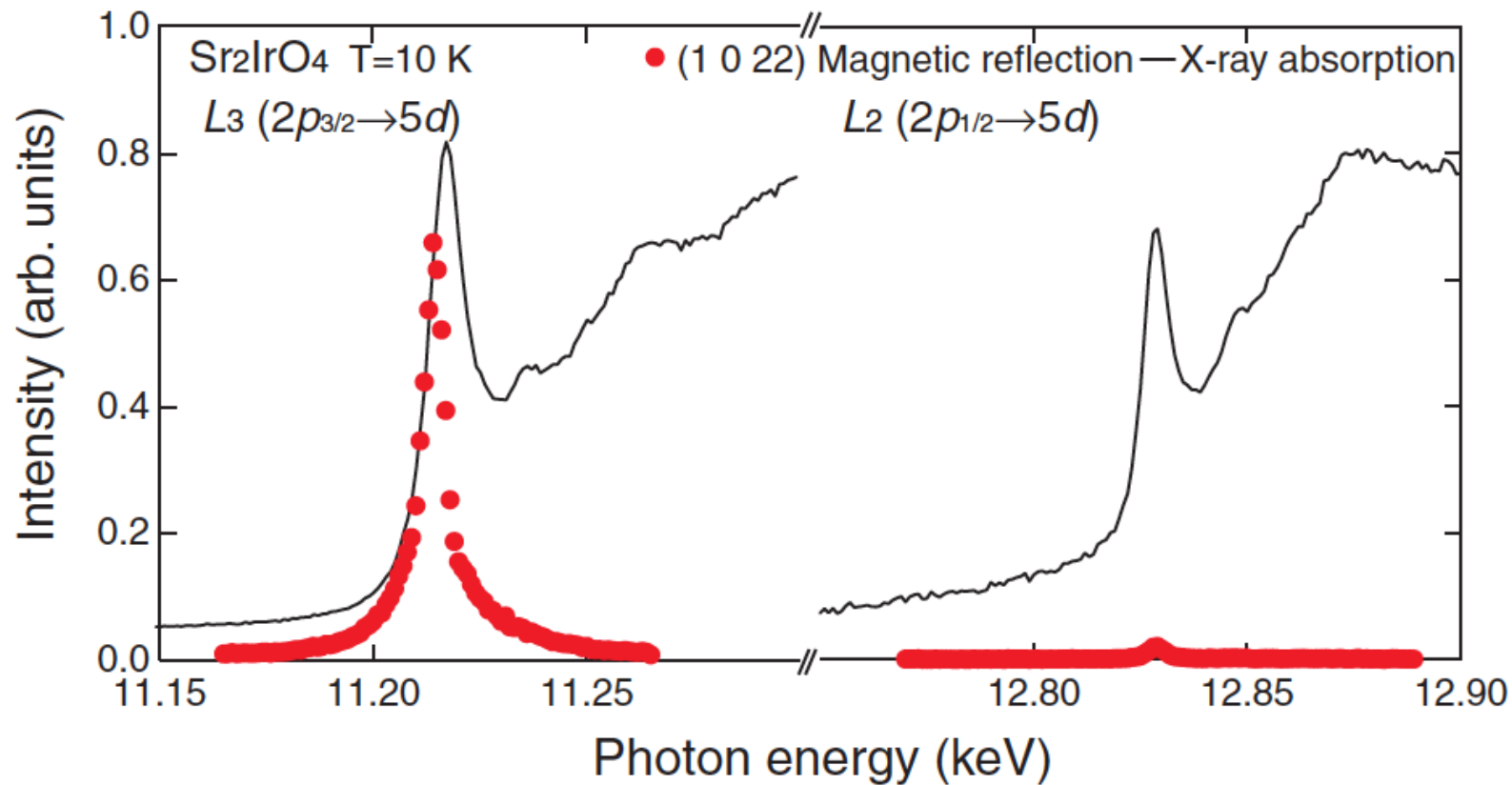
Resonant x-ray scattering contains information about spin and orbital structure of scattering ion

XMCD and RXD on Sr_2IrO_4



RXD
B. J. Kim et al. Science (2009)

Evidence for $J_{\text{eff}}=1/2$ states



Almost no resonance at L_2 :
 L_2 scattering intensity is only about 1% of that of the L_3 .

RIXS cross section

To calculate $O_{l_z, l_{z'}}^{\alpha\beta} = \sum_{j_z} \langle l, l_z | R^\alpha | j, j_z \rangle \langle j, j_z | R^\beta | l, l_{z'} \rangle$

we need $\langle l, l_z | T_q^k | j, j_{z'} \rangle$

 Spherical tensor of rank 1

$$z = T_0^1$$

$$x = -\frac{1}{\sqrt{2}}(T_1^1 - T_{-1}^1)$$

$$y = \frac{1}{\sqrt{2}i}(T_1^1 + T_{-1}^1)$$

$$\langle l = 2, s = 1/2; l_z, s_z | T_q^k | l' = 1, s' = 1/2; j, j_{z'} \rangle$$

$$= \sum_{l_z, s_z} \langle l = 2, s = 1/2; l_z, s_z | T_q^k | l' = 1, s' = 1/2; l_z', s_z' \rangle \underbrace{\langle l' = 1, s' = 1/2; l_z', s_z' | j, j_z \rangle}_{\text{Clebsch-Gordan Coefficient}}$$

$$= \sum_{l_z, s_z} \langle l, s; l_z, s_z | T_q^k | l', s'; l_z', s_z' \rangle \delta_{s_z s_z'} \langle l', s'; l_z', s_z' | j, j_z \rangle$$

$$\propto \sum_{l_z} \langle l, k; l_z', q | j, j_z \rangle \langle l', s'; l_z', s_z | j, j_z \rangle$$



Wigner-Eckart theorem

$$\langle l, l_z | T_q^k | l', l_z' \rangle = \langle l, k; l_z', q | l, k; l, l_z \rangle \frac{\langle l' \parallel T^k \parallel l \rangle}{\sqrt{2l+1}}$$

$J_{\text{eff}}=1/2$ → Experiment
Yes!

Experiment → $J_{\text{eff}}=1/2$?

FAST TRACK COMMUNICATION

The magnetic motif and the wavefunction of Kramers ions in strontium iridate (Sr₂IrO₄)

L C Chapon¹ and S W Lovesey^{1,2}

PRL **112**, 026403 (2014)

PHYSICAL REVIEW LETTERS

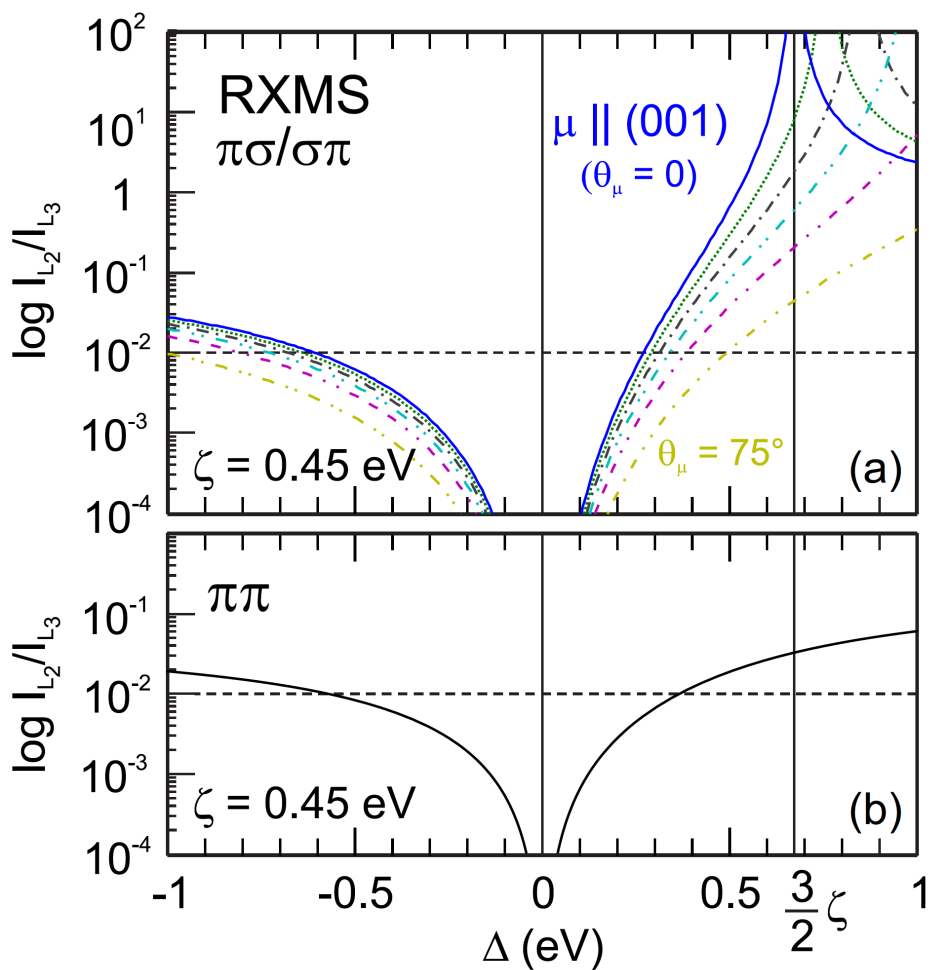
week ending
17 JANUARY 2014

Resonant X-Ray Scattering and the $j_{\text{eff}} = 1/2$ Electronic Ground State in Iridate Perovskites

M. Moretti Sala,^{1,*} S. Boseggia,^{2,3} D. F. McMorrow,^{2,4} and G. Monaco¹

Resonant X-Ray Scattering and the $j_{\text{eff}} = 1/2$ Electronic Ground State in Iridate Perovskites

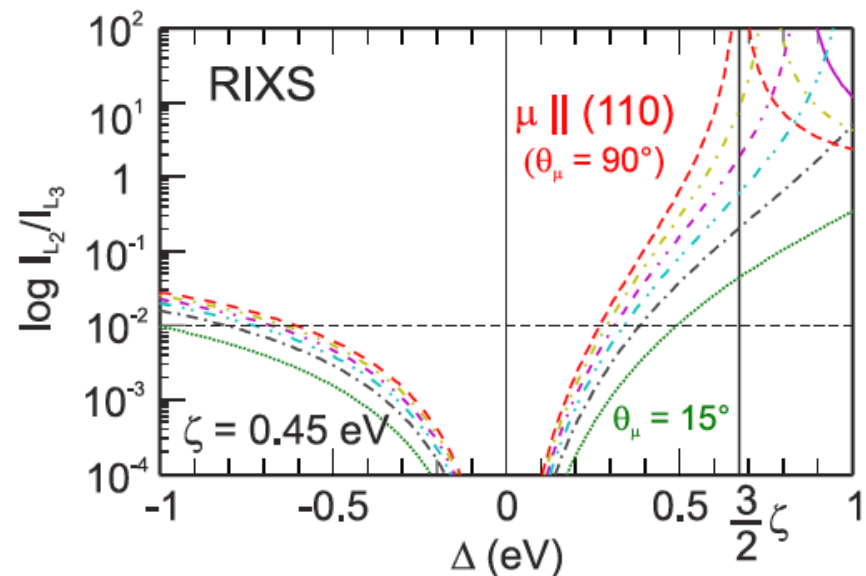
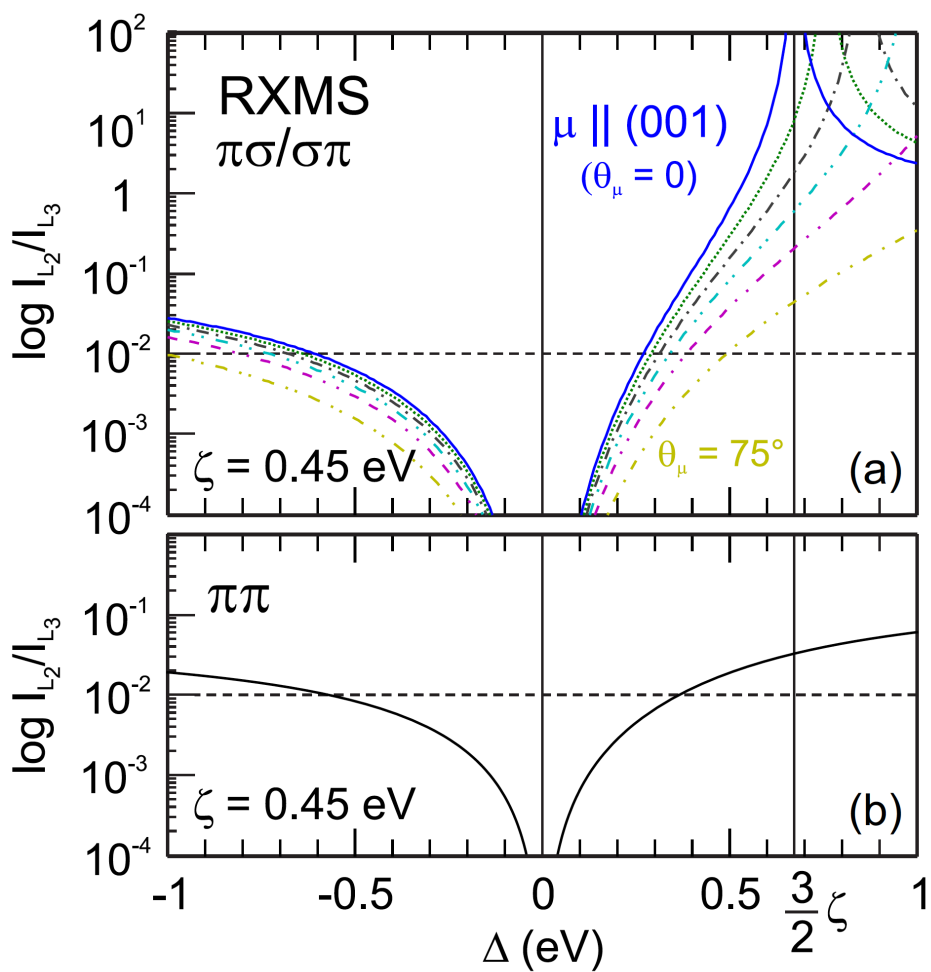
M. Moretti Sala,^{1,*} S. Boseggia,^{2,3} D. F. McMorrow,^{2,4} and G. Monaco¹



- valid only if M is along the axis of distortion (c-axis)
- L_2 intensity vanishes for any Δ if M is in the ab-plane

Resonant X-Ray Scattering and the $j_{\text{eff}} = 1/2$ Electronic Ground State in Iridate Perovskites

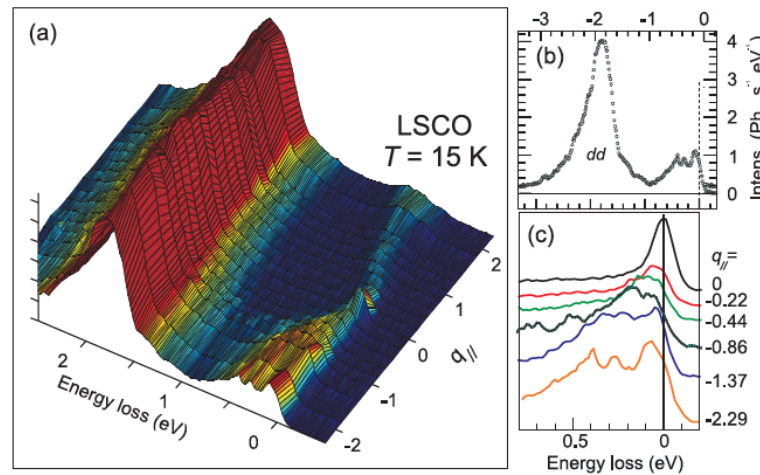
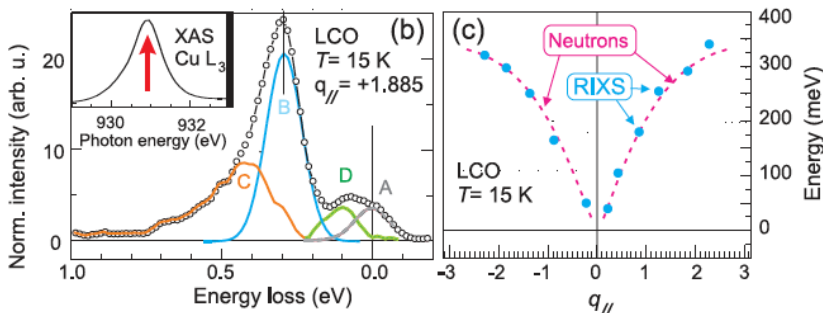
M. Moretti Sala,^{1,*} S. Boseggia,^{2,3} D. F. McMorrow,^{2,4} and G. Monaco¹



RIXS: New Tool to study Magnetic Excitations

soft x-ray (<1 keV)

RIXS experiment on thin film of La_2CuO_4



L. Braicovich et al., PRL (2010)

PRL 103, 117003 (2009)

PHYSICAL REVIEW LETTERS

week ending
11 SEPTEMBER 2009

Theoretical Demonstration of How the Dispersion of Magnetic Excitations in Cuprate Compounds can be Determined Using Resonant Inelastic X-Ray Scattering

Luuk J. P. Ament,^{1,4} Giacomo Ghiringhelli,² Marco Moretti Sala,² Lucio Braicovich,² and Jeroen van den Brink^{1,3,4}

¹Institute-Lorentz for Theoretical Physics, Universiteit Leiden, 2300 RA Leiden, The Netherlands

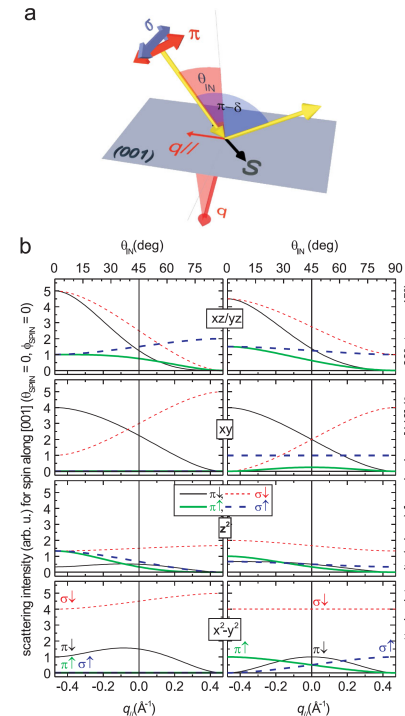
²INFM/CNR Coherentia and Soft-Dipartimento di Fisica, Politecnico di Milano, Piazza Leonardo da Vinci 32, 20133 Milano, Italy

³Institute for Molecules and Materials, Radboud Universiteit, 6500 GL Nijmegen, The Netherlands

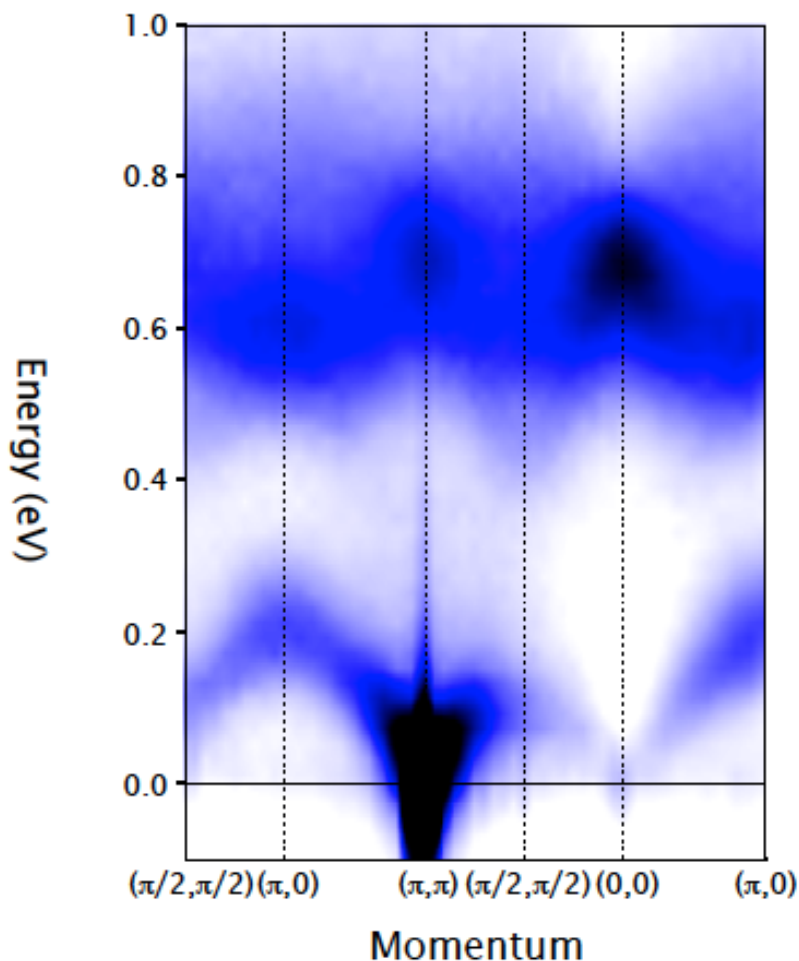
⁴Stanford Institute for Materials and Energy Sciences, Stanford University and SLAC National Accelerator Laboratory, Menlo Park, California 94025, USA

(Received 13 March 2009; published 11 September 2009)

We show that in resonant inelastic x-ray scattering (RIXS) at the copper L and M edge direct spin-flip scattering is in principle allowed. We demonstrate how this possibility can be exploited to probe the dispersion of magnetic excitations, for instance magnons, of cuprates such as the high T_c superconductors. We compute the relevant local and momentum dependent magnetic scattering amplitudes, which we compare to the elastic and dd -excitation scattering intensities. For cuprates these theoretical results put RIXS as a technique on the same footing as neutron scattering.



RIXS: New Tool to study Magnetic Excitations



5d TMO hard x-ray (~11 keV)

2010

our first experiment on iridate
using Si (844) analyzer @ APS
130 meV, 3000 cps

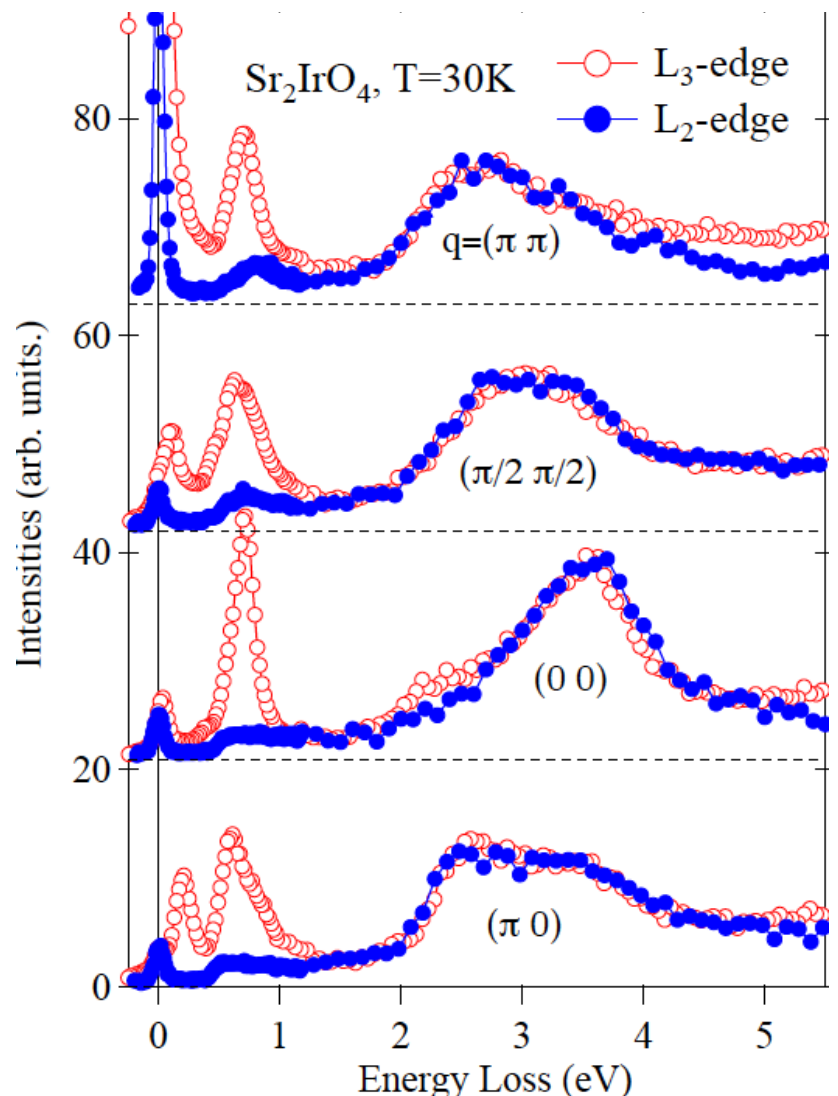
now

25 meV resolution routinely
available at APS and ESRF

2016

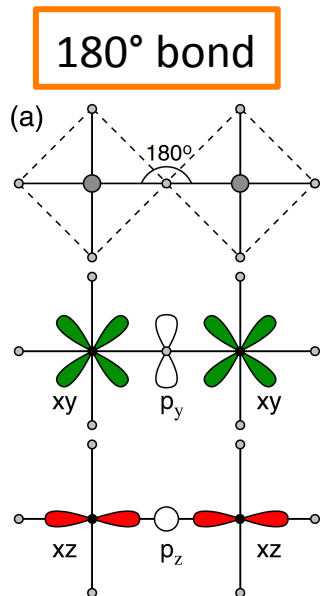
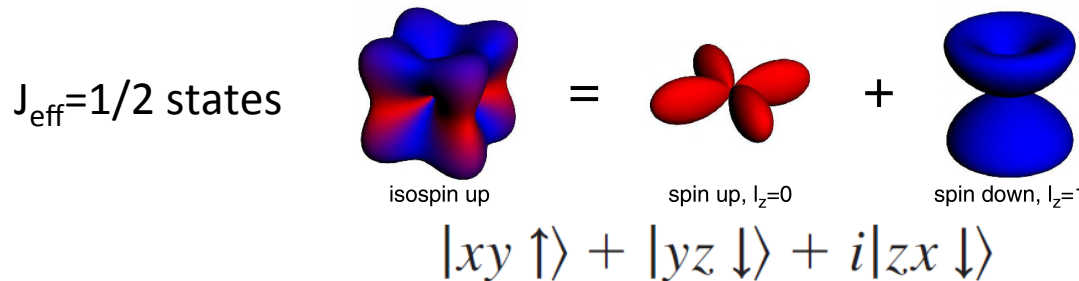
sub 10-meV targeted in
coming years

L2/L3 intensity ratio in RIXS



magnon at L2 edge
suppressed below
detection level!!

Goodenough-Kanamori theory on $J_{\text{eff}}=1/2$ states

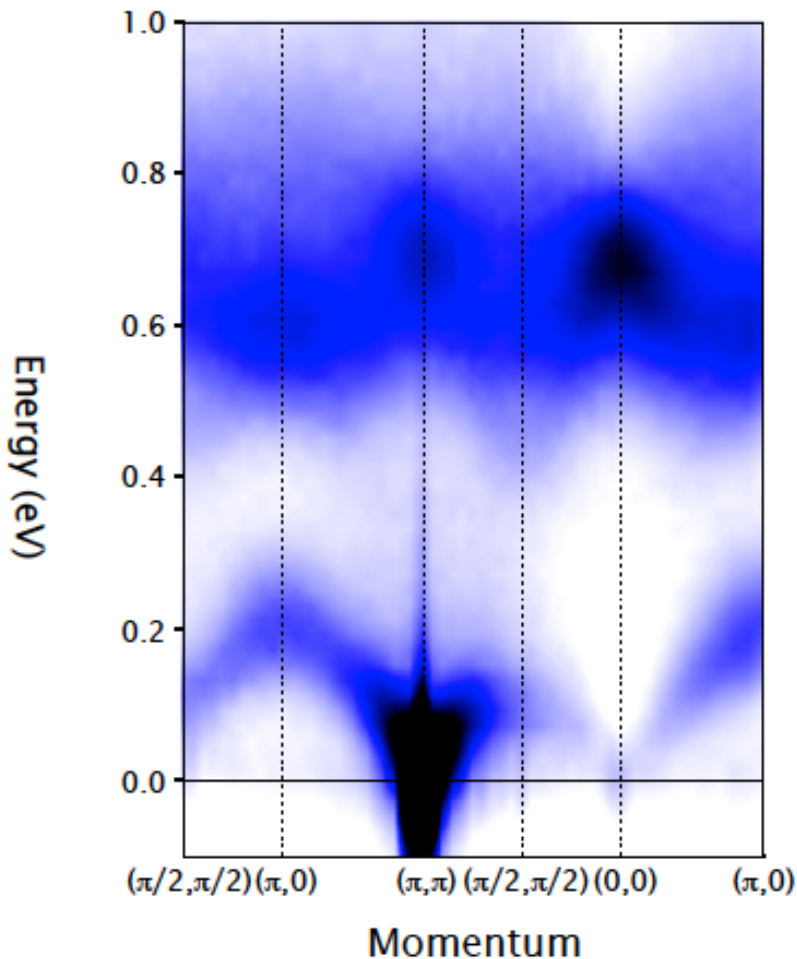


$$\mathcal{H}_{ij} = J_1 \vec{S}_i \cdot \vec{S}_j + J_2 (\vec{S}_i \cdot \vec{r}_{ij})(\vec{r}_{ij} \cdot \vec{S}_j),$$

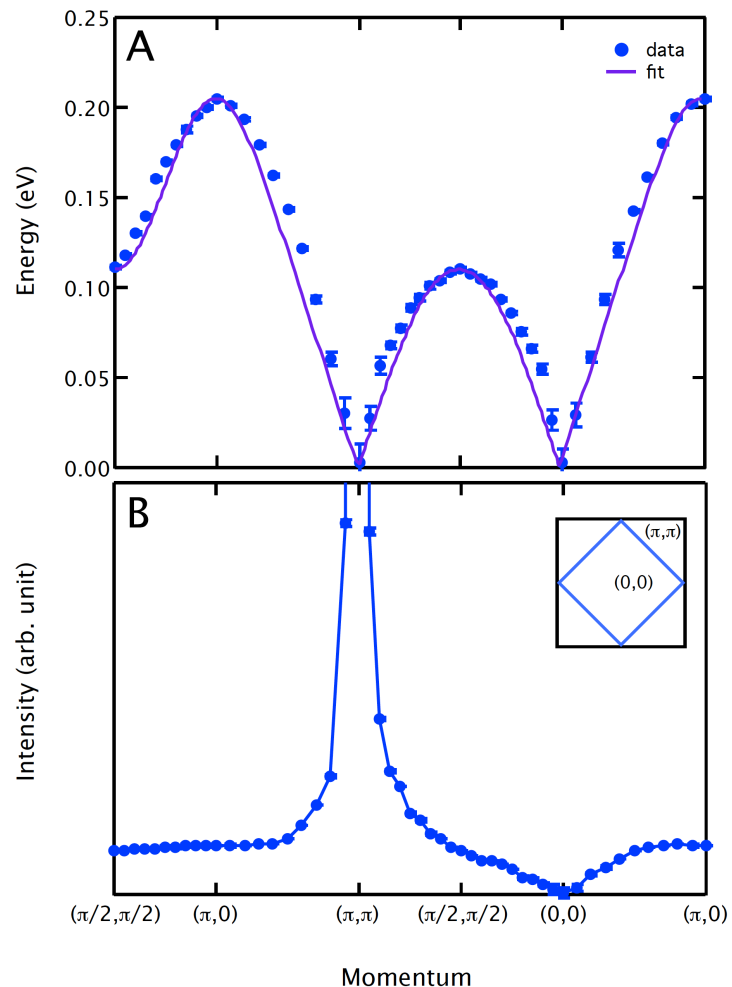
Predominantly
Heisenberg-like
 $J_1 \gg J_2$

Spin wave- fitting to Heisenberg model

2010

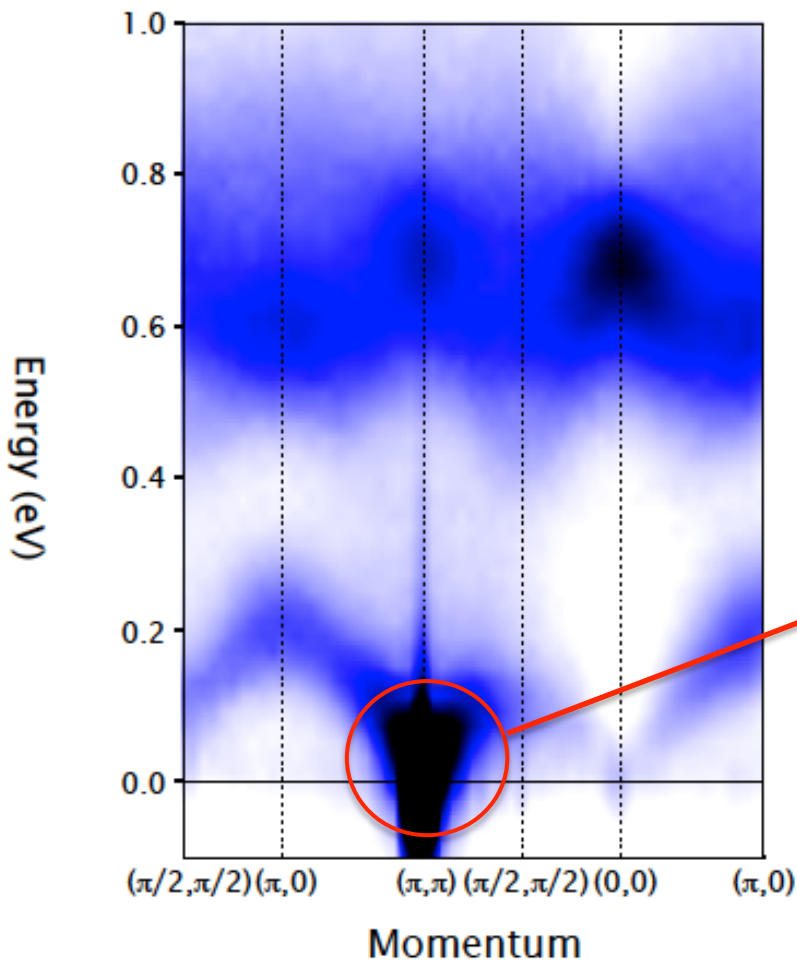


$J=60$
 $J'=-20$
 $J''=15$

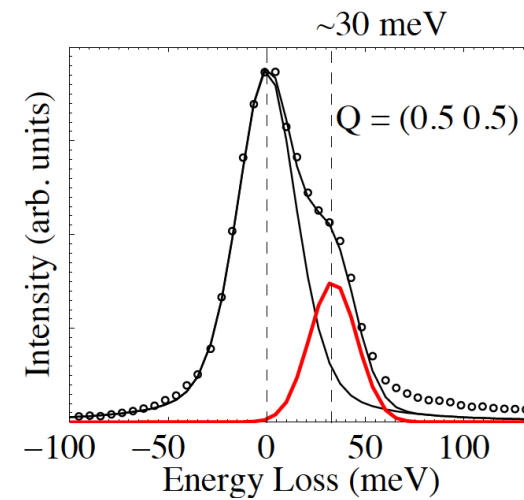


Spin wave gap

2010



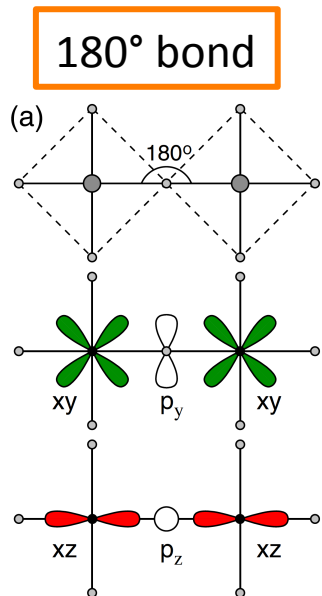
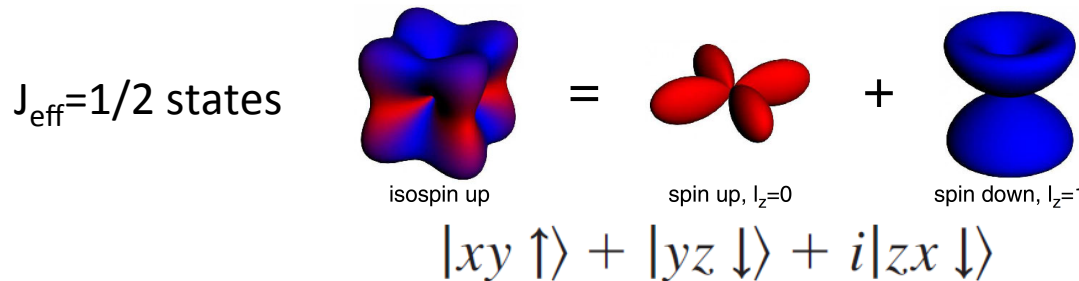
2015



Sizable XY anisotropy!

see also J. Vale et al. PRB (2015)

Goodenough-Kanamori theory on $J_{\text{eff}}=1/2$ states

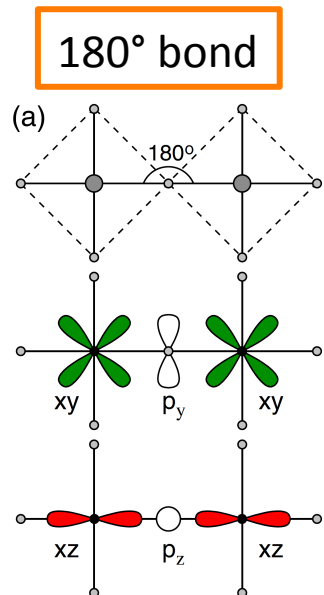
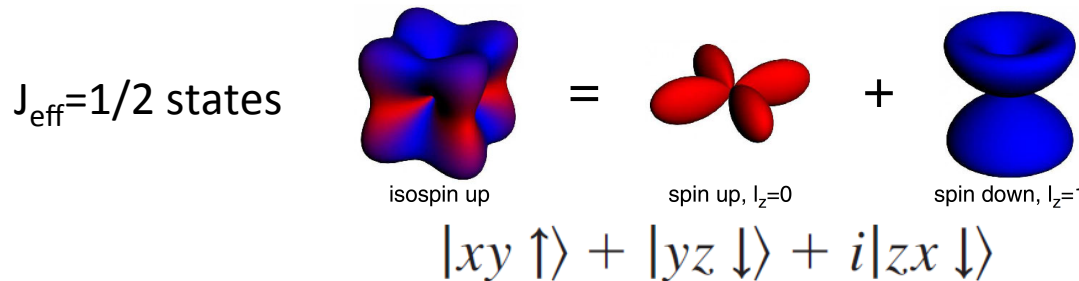


$$\mathcal{H}_{ij} = J_1 \vec{S}_i \cdot \vec{S}_j + J_2 (\vec{S}_i \cdot \vec{r}_{ij})(\vec{r}_{ij} \cdot \vec{S}_j),$$

-Compass
-bond-directional
-Pseudodipolar



Goodenough-Kanamori theory on $J_{\text{eff}}=1/2$ states



$$\mathcal{H}_{ij} = J_1 \vec{S}_i \cdot \vec{S}_j + J_2 (\vec{S}_i \cdot \vec{r}_{ij})(\vec{r}_{ij} \cdot \vec{S}_j),$$

- Compass
- bond-directional
- Pseudodipolar

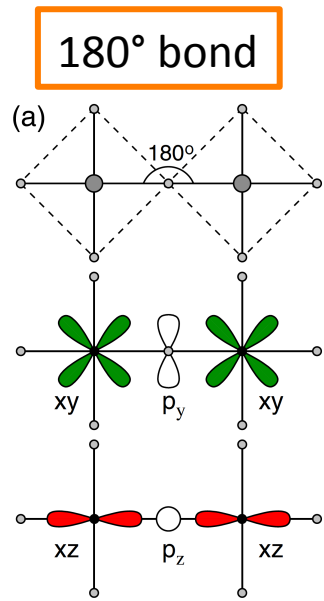


Goodenough-Kanamori theory on $J_{\text{eff}}=1/2$ states

$J_{\text{eff}}=1/2$ states

isospin up = spin up, $l_z=0$ + spin down, $l_z=1$

$$|xy \uparrow\rangle + |yz \downarrow\rangle + i|zx \downarrow\rangle$$



$$\mathcal{H}_{ij} = J_1 \vec{S}_i \cdot \vec{S}_j + J_2 (\vec{S}_i \cdot \vec{r}_{ij})(\vec{r}_{ij} \cdot \vec{S}_j),$$

-Compass
-bond-directional
-Pseudodipolar

responsible for magnetic anisotropy and magnon gap

weak SOC limit: scales with λ
strong SOC limit: scales with J_H/U

Pseudodipolar term in a square lattice



$$\mathcal{H}_{ij} = J_{ij} \vec{S}_i \cdot \vec{S}_j + \Gamma S_i^x S_j^x$$

$$\frac{\Gamma}{2}(S_i^x S_j^x + S_i^y S_j^y) + \frac{\Gamma}{2}(S_i^x S_j^x - S_i^y S_j^y)$$

A_{1g}

B_{1g}

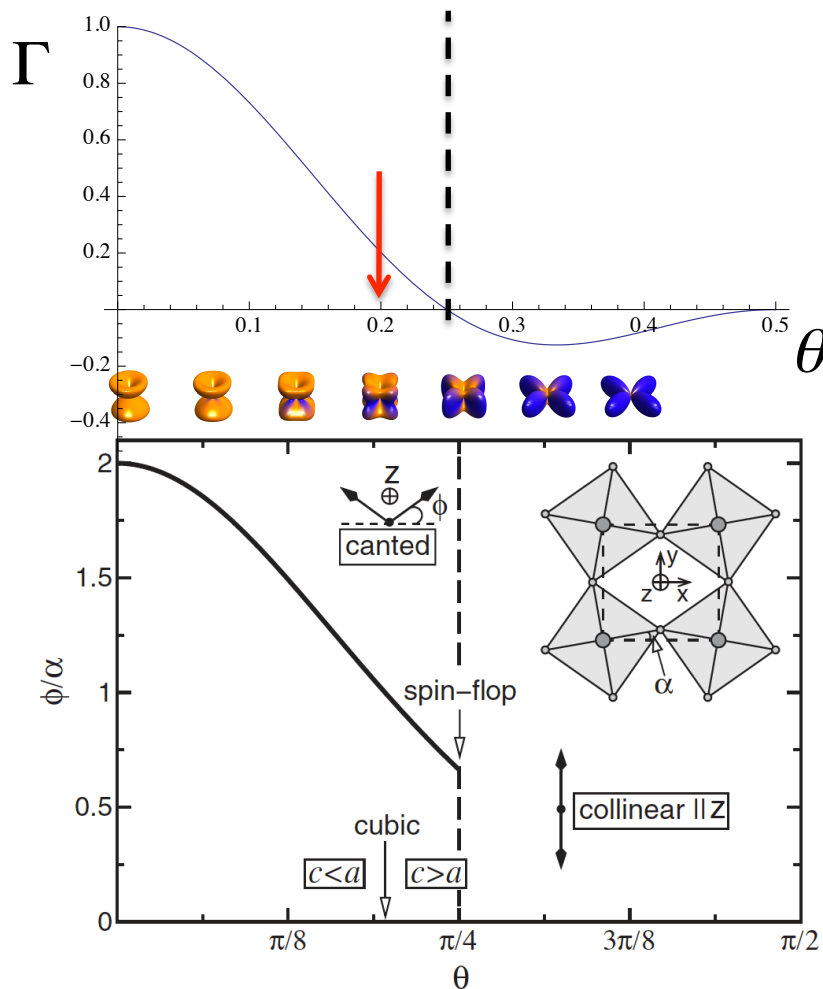


$$\mathcal{H}_{ij} = J_{ij} \vec{S}_i \cdot \vec{S}_j + \Gamma S_i^y S_j^y$$

$$\frac{\Gamma}{2}(S_i^x S_j^x + S_i^y S_j^y) - \frac{\Gamma}{2}(S_i^x S_j^x - S_i^y S_j^y)$$

$$\mathcal{H}_{ij} = (J_{ij} + \Gamma/2) \vec{S}_i \cdot \vec{S}_j - \frac{\Gamma}{2} S_i^z S_j^z$$

Pseudodipolar term in a square lattice

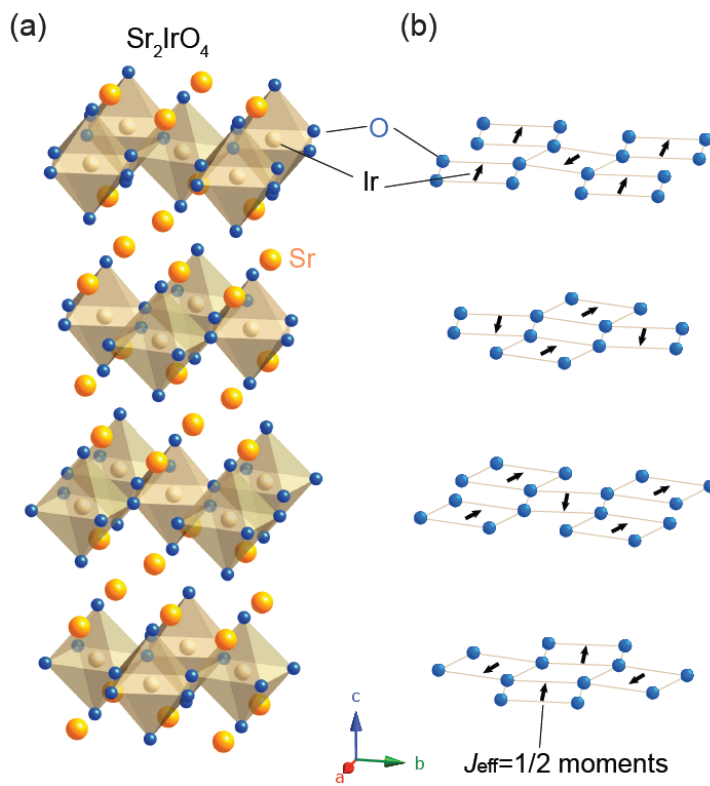


$$\mathcal{H}_{ij} = (J_{ij} + \Gamma/2) \vec{S}_i \cdot \vec{S}_j - \frac{\Gamma}{2} S_i^z S_j^z$$

Ruddelsden-Popper Series Iridates



$T_N=240 \text{ K}$

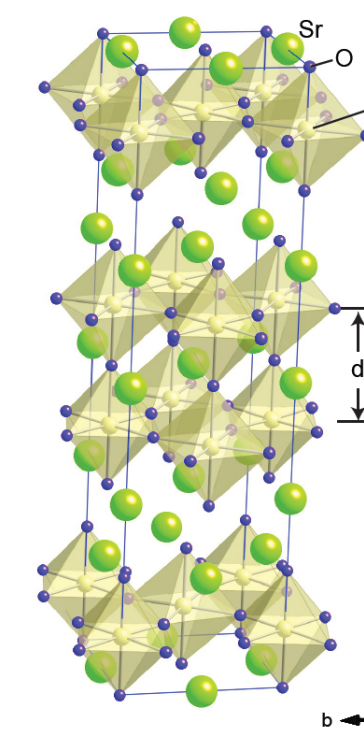


B. J. Kim et al. Science (2009)

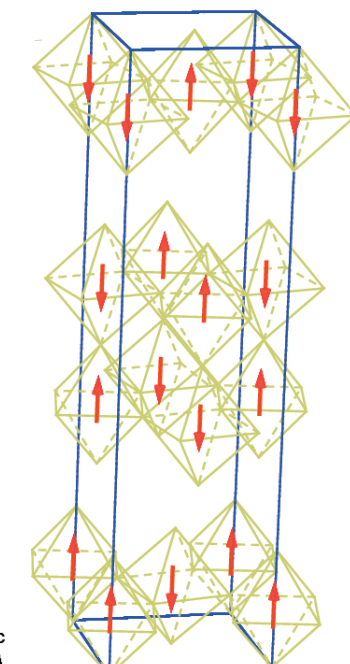


$T_N=285 \text{ K}$

(a)



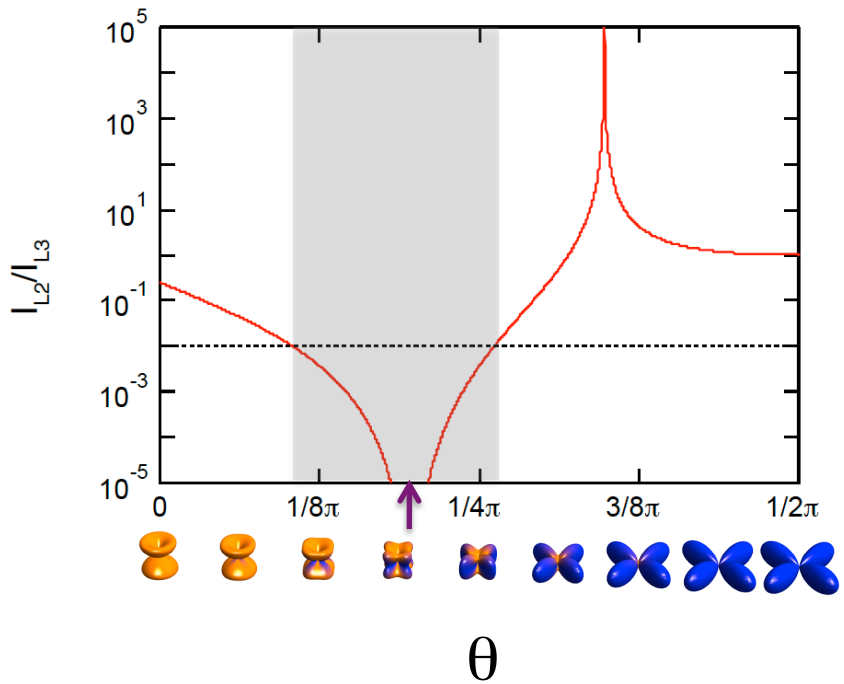
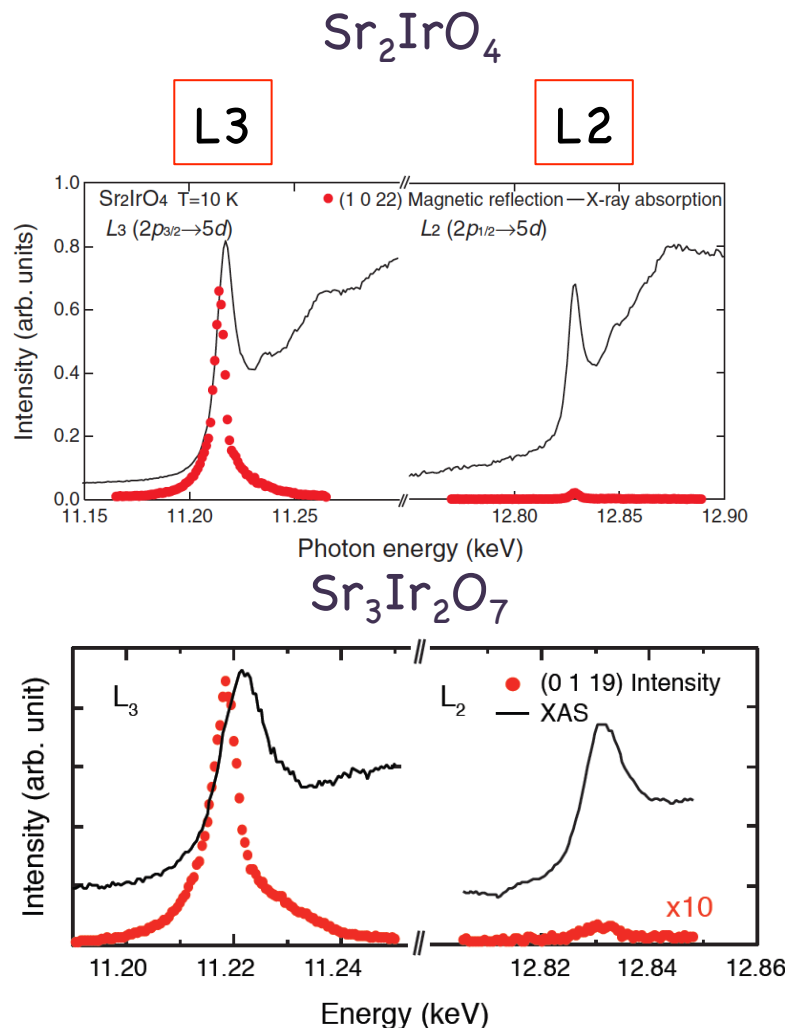
(b)



G-type AF
c-axis collinear

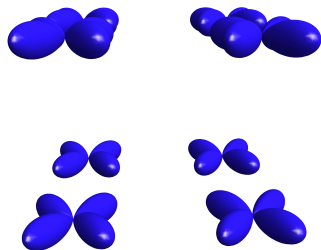
J. -W. Kim, BJK et al. PRL (2012),
S. Boseggia et al, J. Phys. Condens. Matter (2015)
J. P. Clancy et al., arxiv (2012)
S. Fujiyama et al. PRB (2012)

L2/L3 RXD Intensity



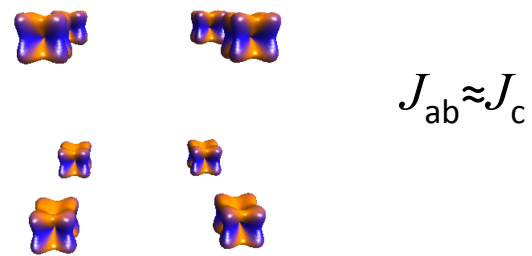
$$\mathcal{H}_{ij} = J_1 \vec{S}_i \cdot \vec{S}_j + J_2 (\vec{S}_i \cdot \vec{r}_{ij})(\vec{r}_{ij} \cdot \vec{S}_j),$$

Orbitals polarized,
anisotropy in superexchange
interactions

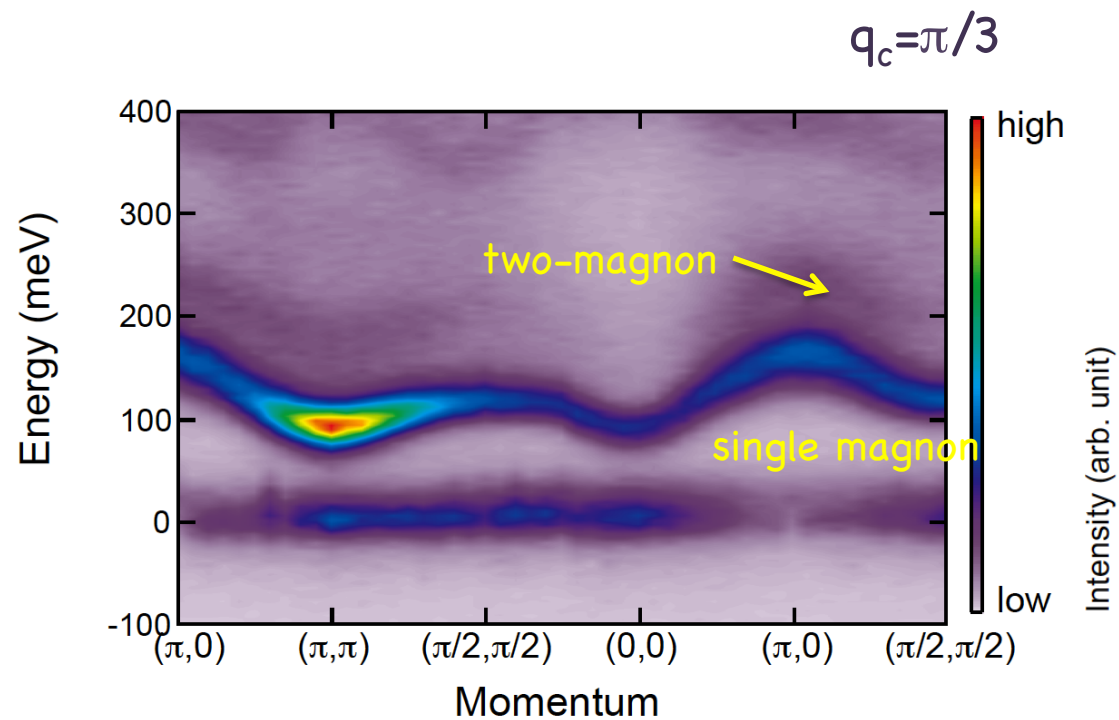


$$J_{ab} \gg J_c,$$

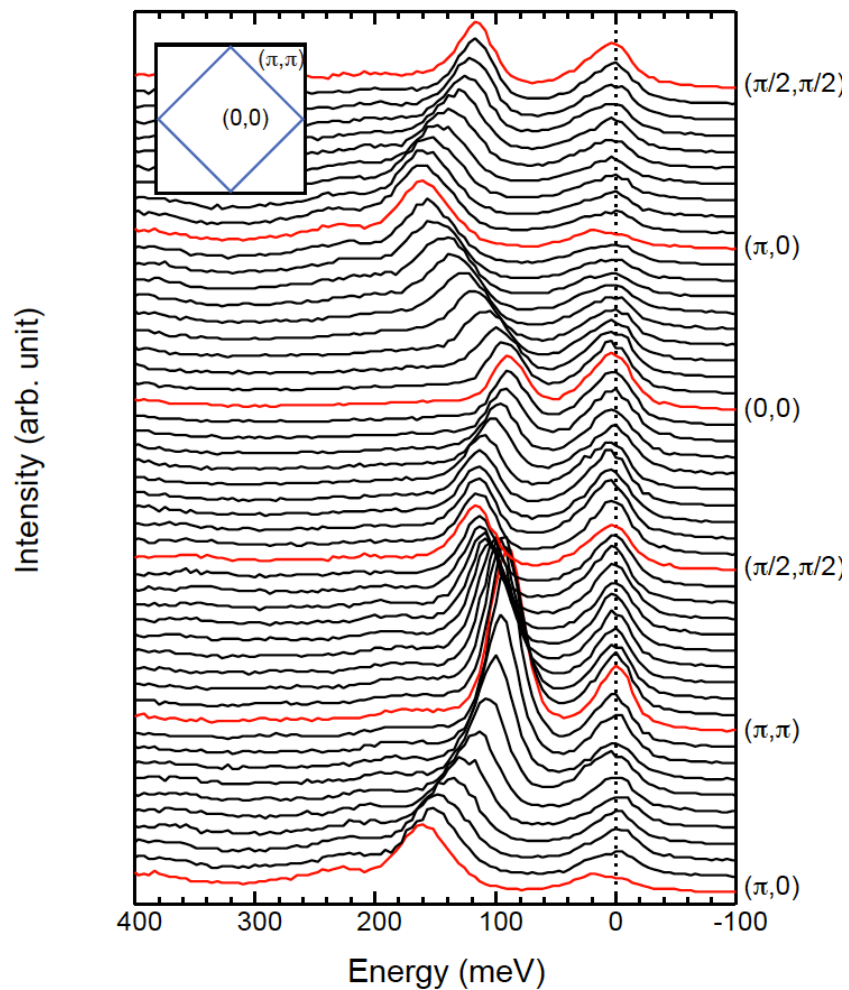
Superexchange interactions
multidirectional



Giant Magnon Gap in $\text{Sr}_3\text{Ir}_2\text{O}_7$



- Large magnon gap $\Delta_m \approx 90$ meV
- Total magnon bandwidth ≈ 70 meV



Optical spectroscopy on RP iridates

$n=1: \text{Sr}_2\text{IrO}_4$

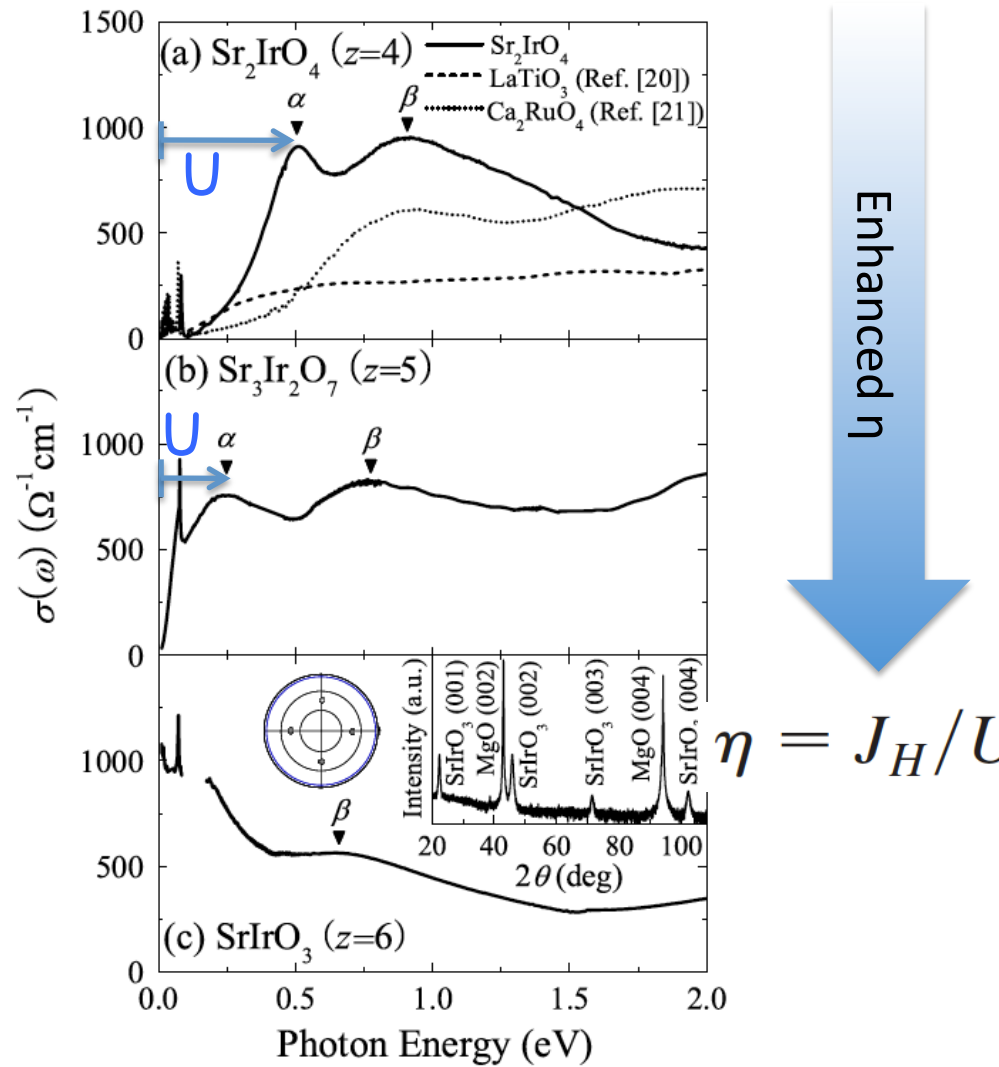
$\Delta_c = 0.35 \text{ eV}$

$n=2: \text{Sr}_3\text{Ir}_2\text{O}_7$

Δ_c very small
(unresolved)

$n=\infty: \text{SrIrO}_3$

metal



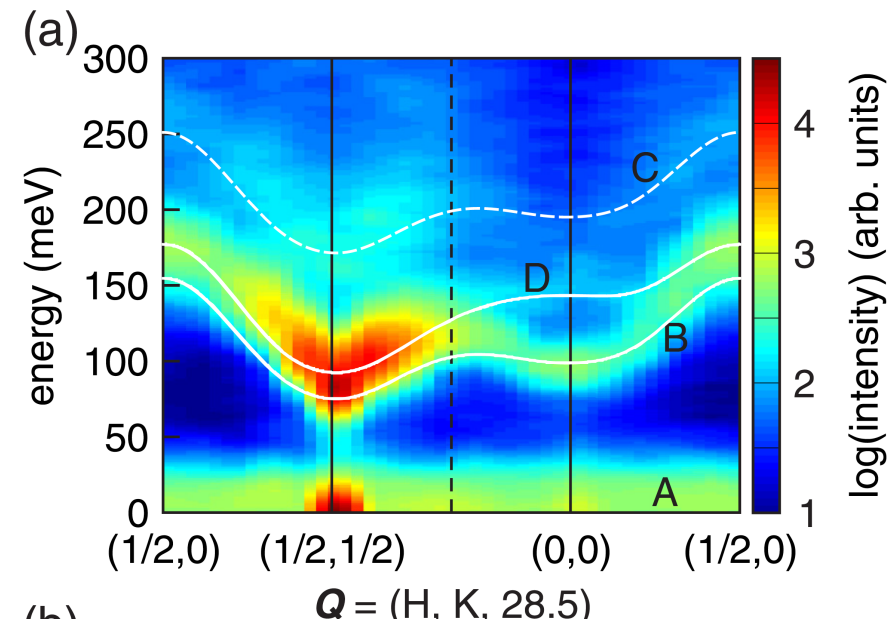
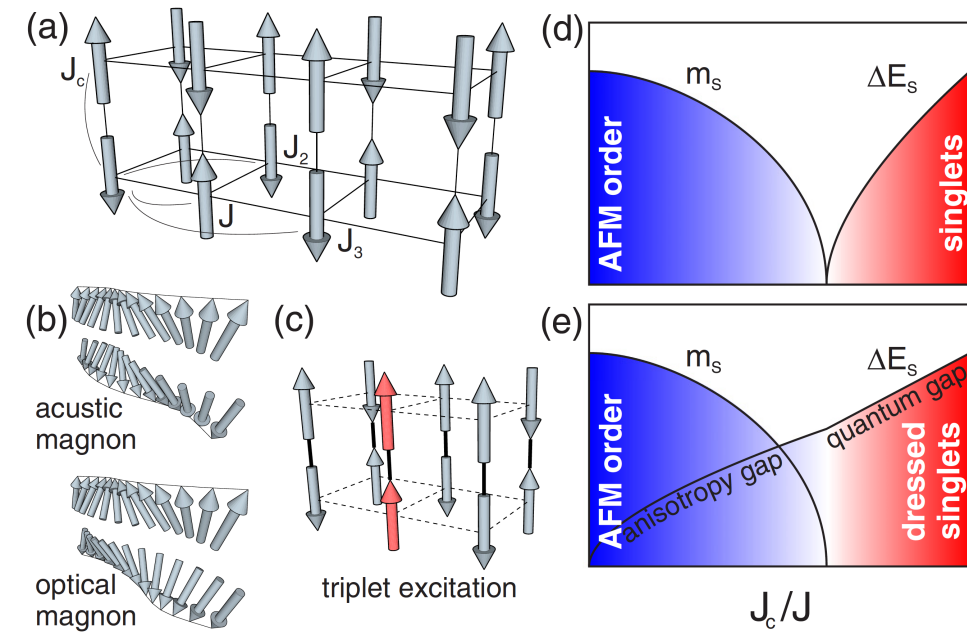
Alternative model

PHYSICAL REVIEW B 92, 024405 (2015)

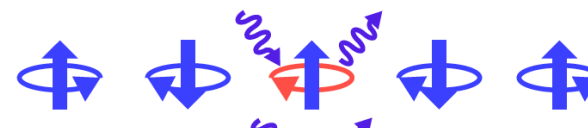
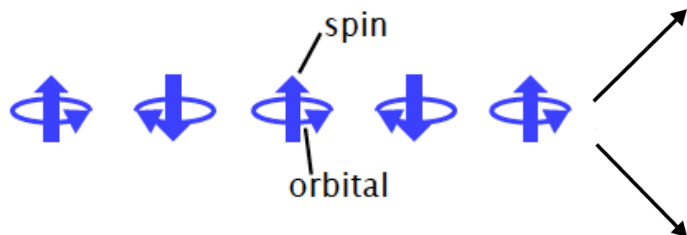
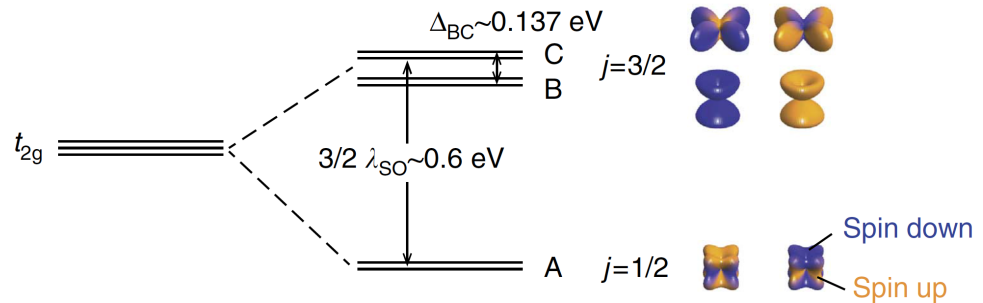
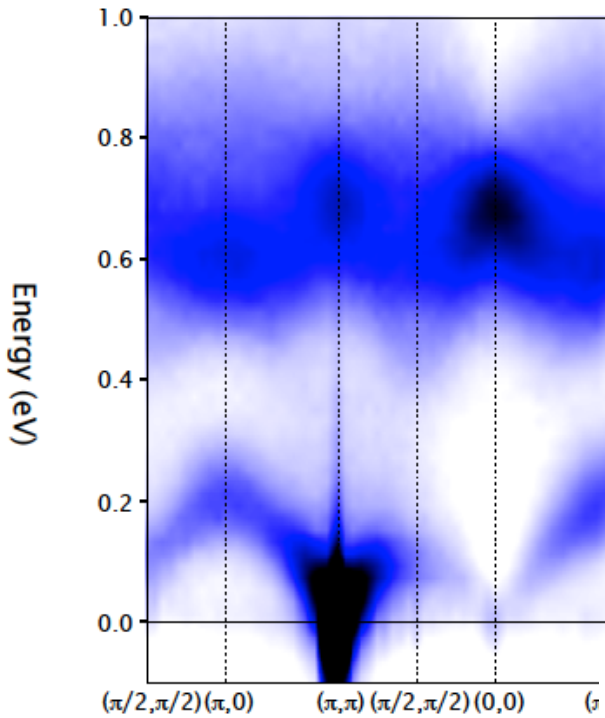
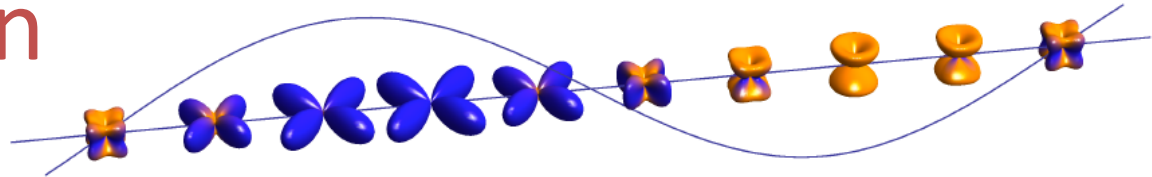


Evidence of quantum dimer excitations in $\text{Sr}_3\text{Ir}_2\text{O}_7$

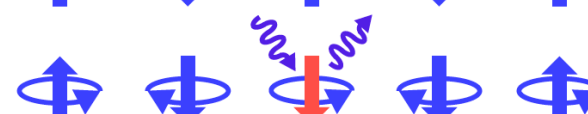
M. Moretti Sala,¹ V. Schnells,² S. Boseggia,^{3,4} L. Simonelli,^{1,5} A. Al-Zein,¹ J. G. Vale,³ L. Paolasini,¹ E. C. Hunter,⁶ R. S. Perry,³ D. Prabhakaran,⁷ A. T. Boothroyd,⁷ M. Krisch,¹ G. Monaco,^{1,8} H. M. Rønnow,^{9,10} D. F. McMorrow,³ and F. Mila¹¹



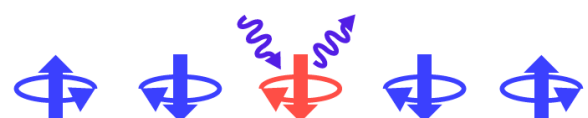
Spin-orbit exciton



orbital flip

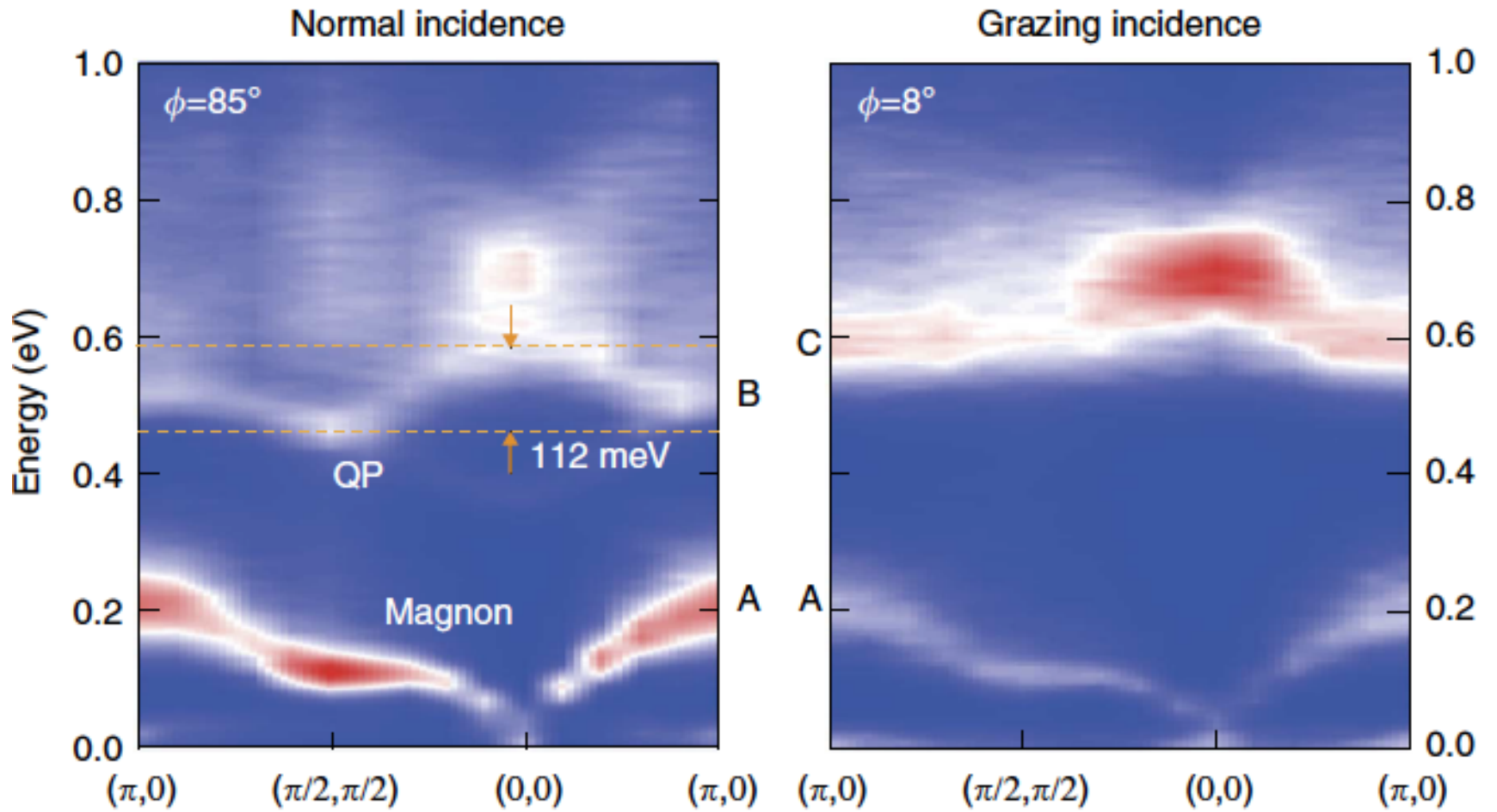
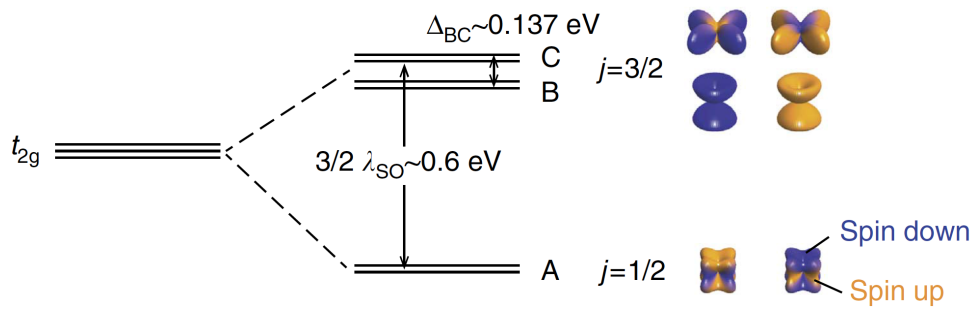


spin flip



spin + orbital flip
scattering

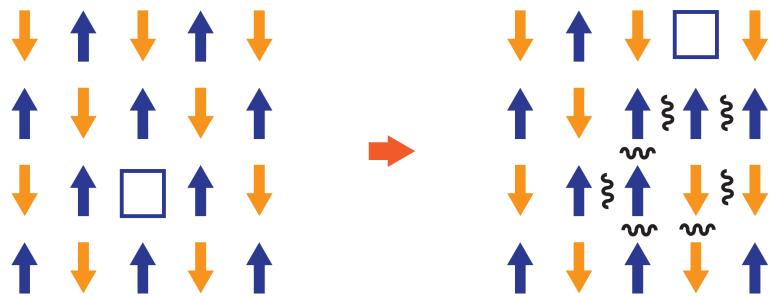
Spin-orbit exciton



One-hole problem

ARPES (photon-in electron-out)

a hole propagation



initial



photon (+ vacuum)

final



photoelectron

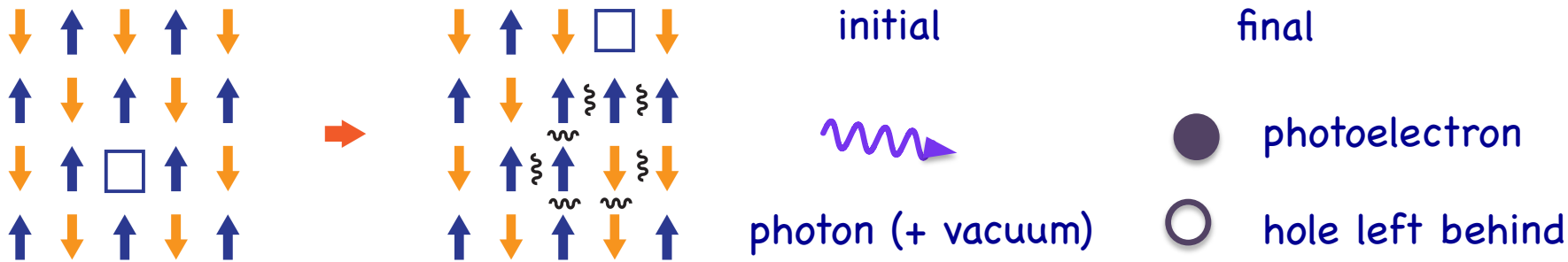


hole left behind

One-hole problem

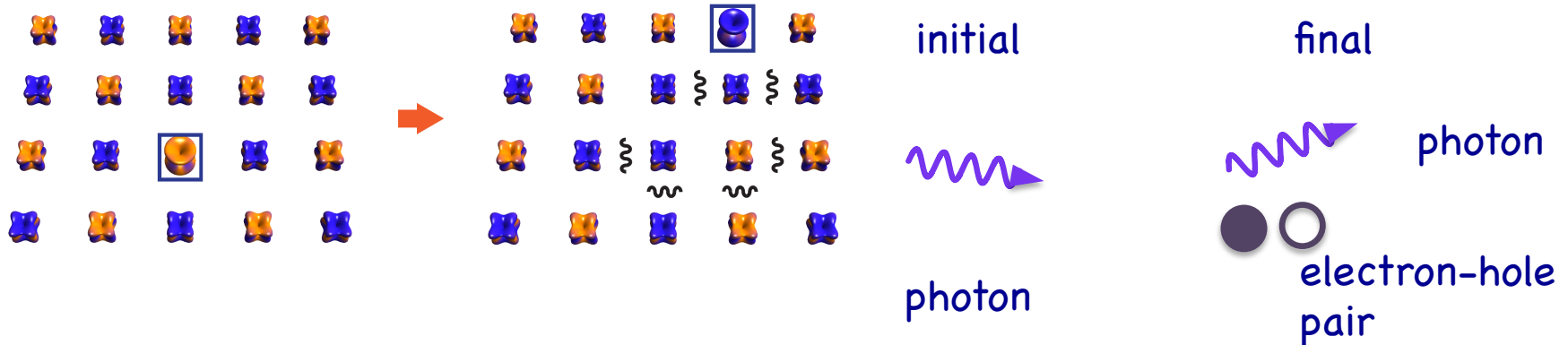
ARPES (photon-in electron-out)

a hole propagation



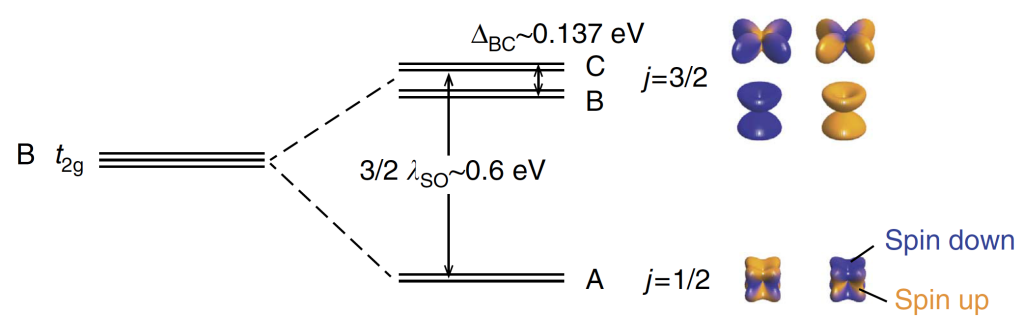
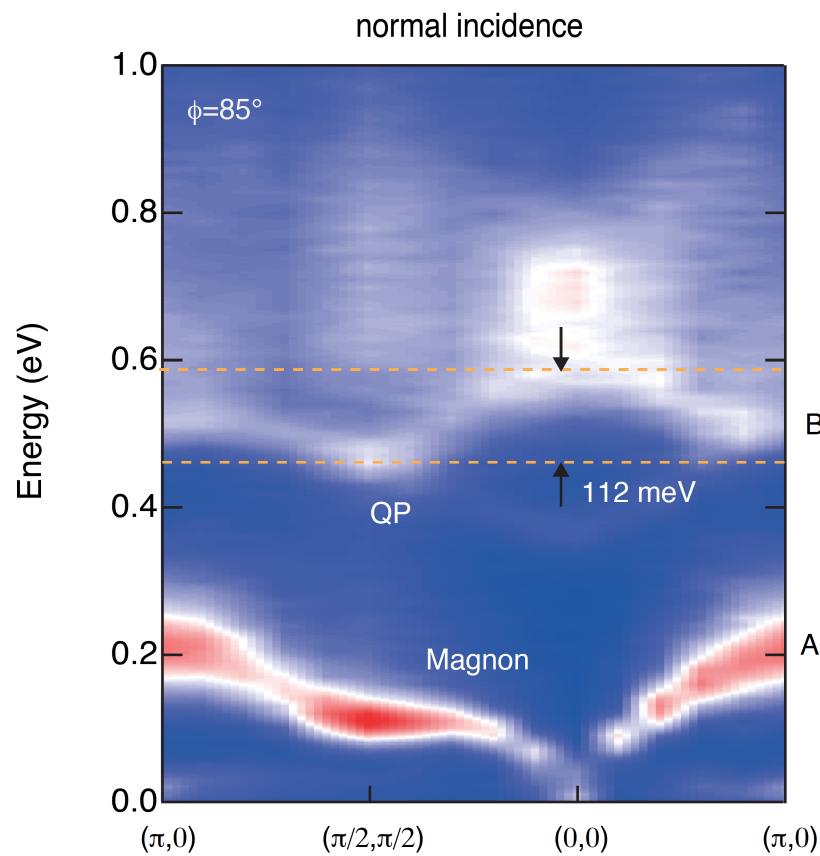
b exciton propagation

RIXS (photon-in photon-out)



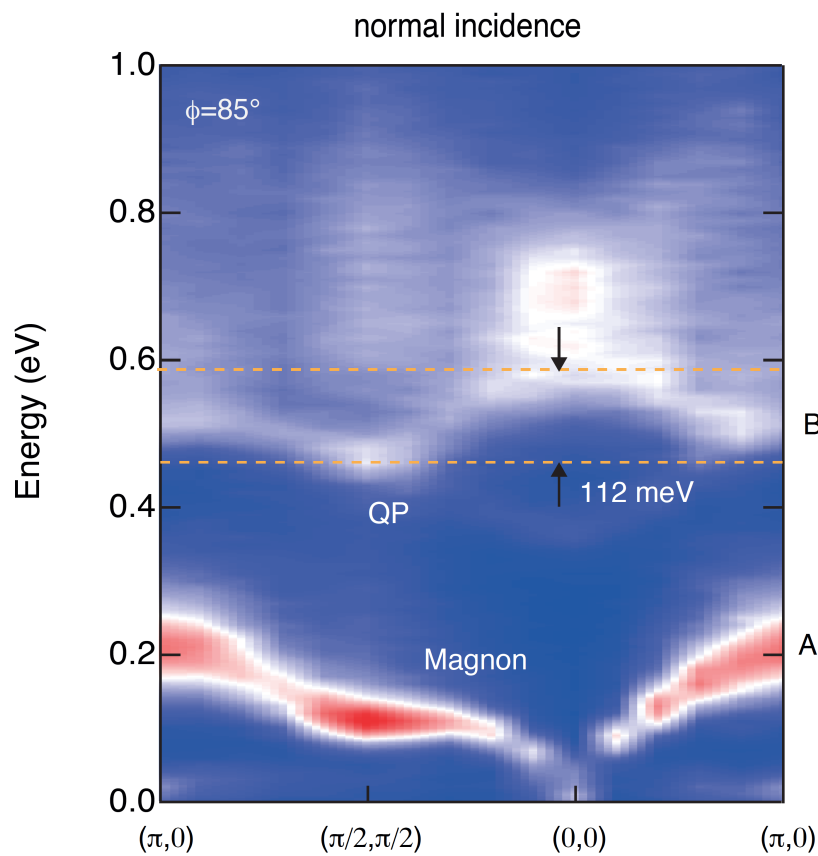
One-hole problem

a RIXS

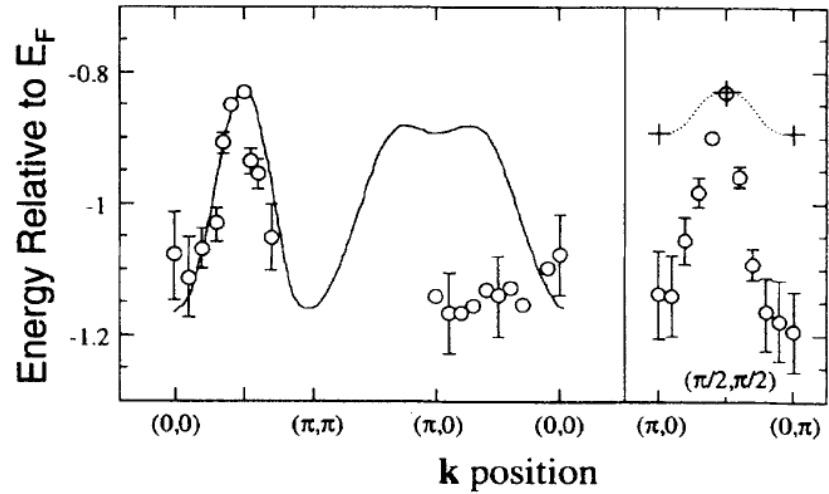


One-hole problem

a RIXS

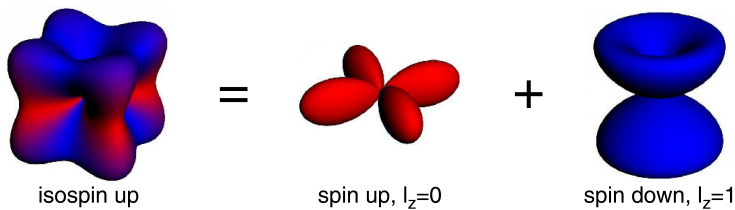


ARPES (cuprate)



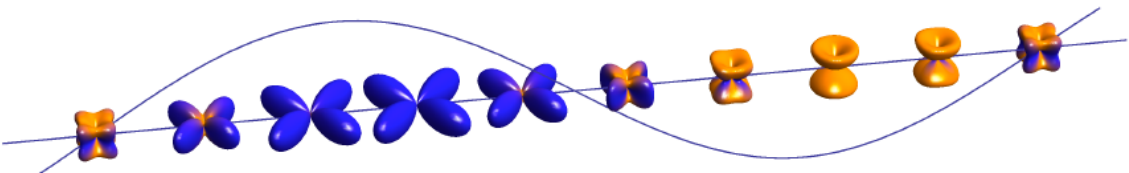
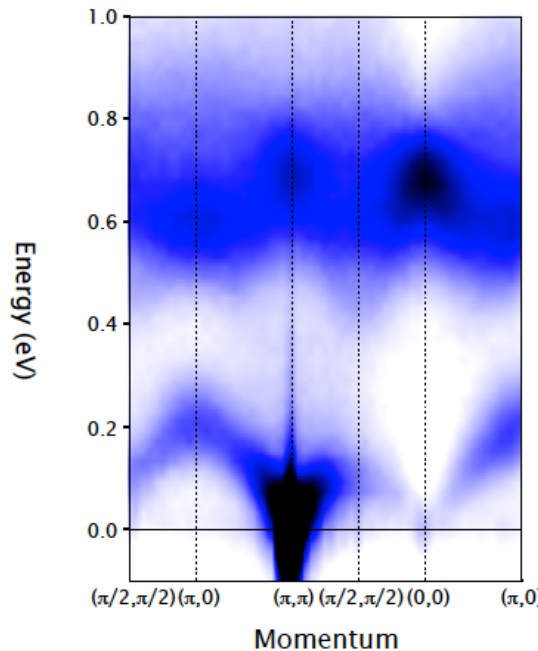
B. O. Wells et al., PRL (1995)

Summary



RXD can not only solve the magnetic structure but also the spin-orbital structure

RIXS is an excellent tool for 5d oxides to study magnetic excitations.



RIXS is sensitive to many other kinds of excitations beyond magnons